

Air Force Institute of Technology

**AFIT Scholar**

---

Theses and Dissertations

Student Graduate Works

---

12-1997

## Photoluminescence Study of GaN Implanted with Erbium and Erbium-Oxygen

Lori R. Everitt

Follow this and additional works at: <https://scholar.afit.edu/etd>



Part of the [Atomic, Molecular and Optical Physics Commons](#)

---

### Recommended Citation

Everitt, Lori R., "Photoluminescence Study of GaN Implanted with Erbium and Erbium-Oxygen" (1997). *Theses and Dissertations*. 5626.  
<https://scholar.afit.edu/etd/5626>

This Thesis is brought to you for free and open access by the Student Graduate Works at AFIT Scholar. It has been accepted for inclusion in Theses and Dissertations by an authorized administrator of AFIT Scholar. For more information, please contact [richard.mansfield@afit.edu](mailto:richard.mansfield@afit.edu).

AFIT/EN/ENP/97D-02

PHOTOLUMINESCENCE STUDY OF GAN  
IMPLANTED WITH ERBIUM AND ERBIUM+OXYGEN

THESIS

Lori R. Everitt,  
Captain, USAF

AFIT/EN/ENP/97D-02

Approved for public release; distribution unlimited

19980121 064

DTIC QUALITY INSPECTED 3

AFIT/EN/ENP/97D-02

PHOTOLUMINESCENCE STUDY OF GAN  
IMPLANTED WITH ERBIUM AND ERBIUM+OXYGEN  
AS A FUNCTION OF EXCITATION WAVELENGTH AND SAMPLE TEMPERATURE

THESIS

Presented to the Faculty of the Graduate School of Engineering

of the Air Force Institute of Technology

Air University

Air Education and Training Command

In Partial Fulfillment of the Requirements for the  
Degree of Master of Science in Engineering Physics

Lori R. Everitt,

Captain, USAF

December 1997

Approved for public release, distribution unlimited

AFIT/EN/ENP/97D-02

PHOTOLUMINESCENCE STUDY OF GAN  
IMPLANTED WITH ERBIUM AND ERBIUM+OXYGEN  
AS A FUNCTION OF EXCITATION WAVELENGTH AND SAMPLE TEMPERATURE

Lori R. Everitt,  
Captain, USAF

Approved:

[Redacted Signature]

Chairman

[Redacted Signature]

\_\_\_\_\_

[Redacted Signature]

12/1/97

Date

1 Dec '97

Date

1 Dec '97

Date

## Table of Contents

<u>Figure</u>	<u>Page</u>
Acknowledgments .....	ii
List of Figures .....	iii
List of Tables .....	iv
Abstract .....	v
I. Introduction.....	I-1
II. Background Theory of Semiconductors .....	II-1
A. What is a Semiconductor?.....	II-1
B. How Does a Semiconductor Emit Photons? .....	II-4
C. How Do Impurities Affect Emissions from Semiconductors?.....	II-5
D. How Do Excitation Wavelength and Temperature Affect the Emissions?.....	II-13
III. Samples, Procedures, and Equipment.....	III-1
A. Samples .....	III-1
B. Procedures.....	III-2
C. Equipment .....	III-4
IV. Results and Discussion.....	IV-1
A. Photoluminescence Spectra of As-Grown GaN .....	IV-1
B. Photoluminescence Spectra of Doped GaN .....	IV-5
C. Effects of Changing the Excitation Wavelength of Doped GaN .....	IV-6
D. Effects of Changing the Sample Temperature of Doped GaN .....	IV-13
E. Comparison of GaN:Er and GaN:Er+O.....	IV-18
V. Conclusion.....	V-1
Appendix A.....	A-1
Appendix B .....	B-1
References .....	R-1
Vita.....	V-1

## Acknowledgments

I am indebted to Dr. Yung Kee Yeo, my thesis advisor; Dr. Robert Hengehold; and Dr. William Bailey, whose guidance and support were invaluable. I would also like to thank Dr. Eric Silkowski because my thesis project would not have been possible without his dissertation or advice. In addition, I am very grateful for Mr. Greg Smith's help. Due to his infinite patience, I learned how to operate the equipment and due to his assistance, my experiments ran well.

Furthermore, I appreciate the technical assistance from my husband, [REDACTED], and the late-night dinners he brought. Lastly, I would like to thank my German shepherd, Einstein, and my toy poodle, Red, for forcing me to take study breaks.

Lori R. Everitt

## List of Figures

<u>Figure</u>	<u>Page</u>
II-1 Schematic Diagram of Energy State Splittings .....	II-2
II-2 Energy Level Diagram of the Valence and Conduction Bands and Bandgap .....	II-3
II-3 Position of ED with Respect to the Conduction Band .....	II-7
II-4 Energy Level Diagram of Four Radiative Recombination Transitions .....	II-8
III-1 Diagram of Face and Back Illumination .....	III-2
III-2 Setup Used to Measure Photoluminescence .....	III-4
IV-1 PMT Spectrum of Lower Energy Transitions in As-Grown GaN .....	IV-2
IV-2 PMT Spectrum of Higher Energy Transitions in As-Grown GaN .....	IV-3
IV-3 PL Spectrum from GaN:Er .....	IV-7
IV-4 1.54- $\mu\text{m}$ PL Spectra of GaN:Er as a Function of Excitation Energy .....	IV-8
IV-5 0.991- $\mu\text{m}$ PL Spectra of GaN:Er as a Function of Excitation Energy .....	IV-9
IV-6 1.54- $\mu\text{m}$ PL Spectra of GaN:Er+O as a Function of Excitation Energy .....	IV-11
IV-7 0.991- $\mu\text{m}$ PL Spectra of GaN:Er+O as a Function of Excitation Energy .....	IV-12
IV-8 1.54- $\mu\text{m}$ PL Spectra of GaN:Er as a Function of Sample Temperature .....	IV-14
IV-9 0.991- $\mu\text{m}$ PL Spectra of GaN:Er as a Function of Sample Temperature .....	IV-15
IV-10 1.54- $\mu\text{m}$ PL Spectra of GaN:Er+O as a Function of Sample Temperature .....	IV-16
IV-11 0.991- $\mu\text{m}$ PL Spectra of GaN:Er+O as a Function of Sample Temperature .....	IV-17

## List of Tables

<u>Table</u>	<u>Page</u>
II-1 Selected Properties of GaN .....	II-4
III-1 List of Equipment Used to Collect Photoluminescence .....	III-7
III-2 Equipment Setting Used to Collect Photoluminescence.....	III-8
IV-1 Experimental Values of the Exciton-Neutral Donor Transition.....	IV-4
IV-2 Experimental Values of the Exciton-Neutral Acceptor Transition ...	IV-4
IV-3 Experimental Values of the Donor-Acceptor, 1 Longitudinal Optical, and 2 Longitudinal Optical Transitions .....	IV-5
IV-4 Integrated Intensity as a Function of Excitation Wavelength.....	IV-18
IV-5 Integrated Intensity as a Function of Sample Temperature .....	IV-19



## Abstract

Erbium (Er) characteristically emits at 1.54  $\mu\text{m}$ , which propagates very well through fiber optic cables. The luminescence from Er in semiconductors must be better understood before it can be used to build faster and more efficient communications systems. This work studies the photoluminescence (PL) from gallium nitride (GaN), GaN implanted with Er alone, and GaN implanted with both Er and oxygen (O) as a function of excitation laser energy and sample temperature. The as-grown GaN was studied first. When the exciton bound to a neutral donor recombined, a photon was emitted at 3.47 eV. A photon emitted at 3.457 eV may have been evidence of the recombination of an exciton bound to a neutral acceptor. Second, Er ion-implanted GaN samples were examined. The Er-ion transitions were observed in two groups around 0.805 and 1.25 eV (1.54 and 0.991  $\mu\text{m}$ ). The PL intensity was measured at four laser excitation wavelengths of 275.4-305.5, 333.6-363.8, 488.0, and 514.5 nm from an Ar-ion laser. Although the PL intensities from GaN:Er were strongest when the sample was excited by the 275.4-305.5 nm multiline, the PL emissions from GaN:Er+O were strongest when excited with the 333.6-364.8 nm line. Regardless, both above and below bandgap laser lines induced strong PL intensities. Last, PL from the two samples was also studied as temperature was increased from 2 to 150 K. In general, the intensities of most peaks decreased as temperature was raised in both samples, but the PL signals persist even at 150 K.

PHOTOLUMINESCENCE STUDY OF GAN  
IMPLANTED WITH ERBIUM AND ERBIUM+OXYGEN  
AS A FUNCTION OF EXCITATION WAVELENGTH AND SAMPLE TEMPERATURE

**I. Introduction**

The United States Air Force needs blue and ultraviolet (UV) optoelectronic devices to maintain technological superiority because these devices can be used to build faster and more efficient communications systems which are also resistant to electronic countermeasures and to EMP radiation; detectors which can withstand solar radiation; high density optical data storage devices; secure links between the Earth and its satellites; and aircraft or automobile engine detectors. In particular, Group III-nitrides such as GaN, AlGaN, and InGaN are important semiconductors since they could be used to make optoelectronic devices that emit at wavelengths ranging from the visible to the deep UV region of the spectrum. GaN is a wide bandgap semiconductor, which makes it very promising as a host semiconductor for room temperature rare earth (RE) luminescent devices. Erbium (Er) is worth studying because it emits at 1.54  $\mu\text{m}$ , which propagates well in silicon-based optical fibers. Furthermore, oxygen (O) enhances the Er signal when both are implanted into AlGaAs. This work determined if O enhances the Er signal in GaN.

Several researchers have already used group III-nitrides to make several types of semiconductor devices such as LEDs, UV detectors, UV injection lasers, and field effect transistors (FET's). Carrano reported a UV photodetector made from GaN (Carrano,

1997:1992). In addition, Nakamura reported a GaN-based UV injection laser (Im, 1997:631). Lastly, Khan made a FET from GaN (Ishikawa, 1997:1315).

Current research efforts are directed towards the development of LEDs and laser diodes from Er-implanted GaN. GaN is being used to make many types of devices and it is necessary to understand more about how the Er ions in this semiconductor behave. Silkowski studied light emitted from GaN implanted with several ion species including Er as a function of excitation energy and temperature (Silkowski, 1996:xviii). This thesis work extended Silkowski's efforts. The purpose of this work was to study the effects of excitation energy and sample temperature on the intensity of the light from GaN implanted with Er alone and co-implanted with Er and O to determine whether the emissions from the implanted GaN samples is strong enough to be used in optoelectronic devices, including LEDs and laser diodes.

This thesis report consists of six chapters. Chapter I is an introduction and Chapter II provides some background theory to help the reader to understand the results. Chapters III and IV are the heart of the document, which describe the equipment, procedures, samples, and results of the experiment. The summary is given in Chapter V and recommendations are made in Chapter VI.

## **II. Background Theory of Semiconductors**

As stated in the introduction, the US Air Force needs semiconductor materials which can emit at specific wavelengths which depend on the application. When building a semiconductor device, it is important to understand its emissions and how to improve them. Chapter II describes four concepts which are necessary to understand emissions from a semiconductor. These essential concepts are what is a semiconductor, how does it emit photons, how do impurities affect emissions from a host semiconductor, and how do changes in excitation wavelength and temperature affect the emissions?

### **A. What is a semiconductor?**

The first essential concept is the definition of a semiconductor and its associated energy bands. Since the behavior of the valence electrons explains many optical, electrical, and other physical properties of a semiconductor, understanding it is vital to this work. Each type of atom has a set of characteristic energy states, which depend on the electron configuration of the valence electrons. When atoms are far apart, each atom has the same set of energy states if they are all the same type of atom. However, when the same atoms are brought close enough, the Pauli exclusion principle and the Coulombic repulsion between the valence electrons force the valence electrons into many similar, but slightly different energy states. These energy states appear to split and form an energy band, as shown in Fig II-1. Furthermore, once the energy states start to split, they continue to spread apart as the atoms are brought closer together. The outermost

electrons split first, the second outermost shell splits second, etc., until the interatomic distance becomes stable. The atomic separation stabilizes when the Coulombic attraction between atoms and between the valence electrons of one atom and the nucleus of the other atom balances the

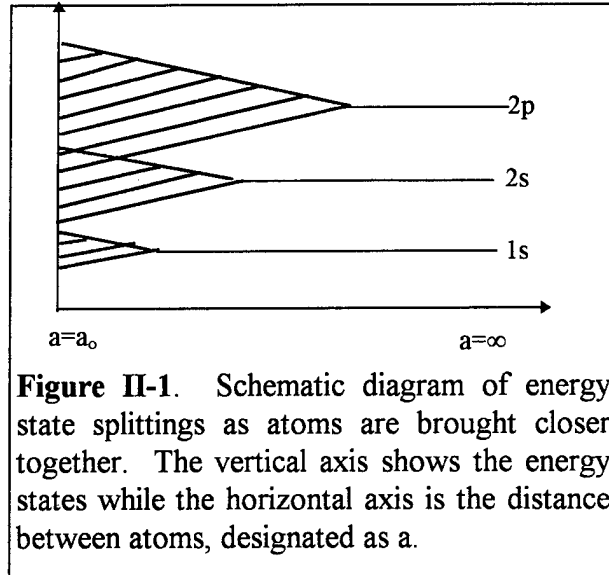
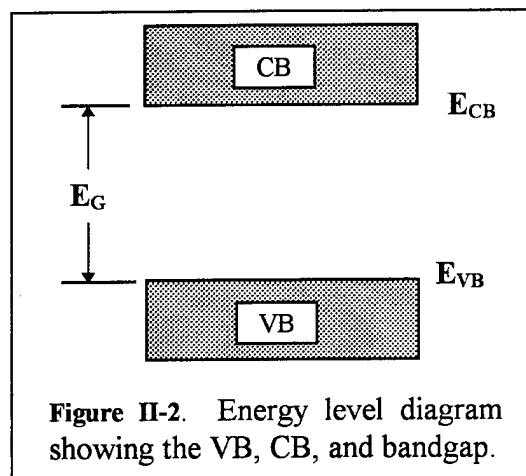


**Figure II-1.** Schematic diagram of energy state splittings as atoms are brought closer together. The vertical axis shows the energy states while the horizontal axis is the distance between atoms, designated as  $a$ .

Coulombic repulsion of the valence electrons associated with each atom. When the interatomic distance is stable, the Coulombic attraction between the atoms is much less than when the atoms were far apart and the final boundaries on the energy states are established. Since the energy state boundaries depend only on the type of atom and the stable interatomic distance, they do not change with respect to the number of atoms.

As more atoms become part of the lattice, the energy states become so tightly packed that they form energy bands. The valence band (VB) is the highest filled energy band and the conduction band (CB) is the band that is just above the VB. The upper boundary of the VB is denoted as  $E_{VB}$  while the lower bound of the CB is designated as  $E_{CB}$ . The VB is the band associated with the outermost electrons when they are in their ground state. Electrons in the CB are free to move around within the CB, forming current, because they feel no influence from an atom in the crystal lattice and there are many empty energy levels into which they can move. The region between the VB and CB is called the bandgap or energy gap and is often designated as  $E_G$ . These bands and the bandgap are depicted in the energy level diagram in Fig. II-2.

An insulator has a large bandgap, about 6 eV, so electrons in the VB cannot be excited into the CB. However, in a semiconductor, the bandgap is smaller, about 3.5 eV for GaN at 0 K. At 0 K, all electrons in a semiconductor occupy energy states within the VB. Since no electrons are in the CB, no current flows, and



the semiconductor behaves as an insulator. But, at higher temperatures, some electrons can be thermally excited into the lower energy states of the CB and current will flow. As temperature increases, more electrons can jump the bandgap resulting in more current. When an electron is excited out of the VB, it leaves behind a hole. A hole is the vacancy that an electron leaves behind in the VB when it is excited to a higher energy state.

Table II-1 lists several selected known properties of GaN, which is the semiconductor used in this thesis experiment. Different researchers may prepare GaN under different conditions and the values of properties can change slightly when this occurs, so be cautious when comparing the properties in Table II-1 to values found in other sources.

**Table II-1. Selected Properties of GaN**

Property Name	Property Value
Crystal Structure	Wurtzite
Direct/Indirect	Direct
Bandgap (eV)	
T $\approx$ 0 K	3.5
T $\approx$ 300 K	3.39
Lattice Constants ( $\text{\AA}$ )	
a	3.189
c	5.185
Density ( $\text{g/cm}^3$ )	6.10
Mobility ( $\text{cm}^2/\text{Vs}$ )	
electrons	440
holes	400
Electron Affective Mass/Electron Rest Mass	0.2
Hole Affective Mass	0.8
Thermal Conductivity ( $\text{W/cm K @300 K}$ )	1.3
Index of Refraction	2.33-2.67
Dielectric Constant	9.5
Melting Point (K)	1500

### B. How Does a Semiconductor Emit Photons?

A semiconductor can emit photons, which can be detected and plotted in spectra. This section describes the process of photon emission in a pure semiconductor. Electrons in the CB will tumble down to the VB after about  $10^{-9}$  sec in a process known as recombination. Luminescence is the light emitted from a semiconductor as electron-hole pairs recombine and emit photons. When a laser beam impinges on a semiconductor, the energy from the beam excites the electrons and creates holes. When these electrons relax, they emit photons. The photons appear as sharp lines in luminescence spectrum at wavelengths corresponding to the change in energy as an electron de-excites from a higher

energy state to a lower energy state. Note, the photon energy is related to the wavelength of the emitted photon by the relation

$$E(eV) = \frac{hc}{\lambda} = \frac{1239.89}{\lambda(nm)}, \quad (1)$$

where E is the photon energy in eV, h is Planck's constant, c is the speed of light, and  $\lambda$  is the wavelength (in nm) of the emitted photon. By measuring the wavelength of the photon, these electronic transitions can be identified. Characteristic Er emissions occur in two groups near 1.54  $\mu\text{m}$  and near 1.00  $\mu\text{m}$  which correspond to the transitions from the  $^4I_{13/2}^1$  manifold to the  $^4I_{15/2}$  energy state (ground state) and the  $^4I_{11/2}$  manifold to the ground state, respectively (Silkowski, 1996:5-136).

### C. How Do Impurities Affect Emissions from Semiconductors?

Part C discusses what are impurities, one method of inserting an impurity into a host semiconductor, how impurities add energy states in the host crystal, and recombination processes associated with semiconductors.

An impurity is an element that is implanted in the host crystal to modify electrical or optical properties of the semiconductor. An impurity is unique in that it can be added intentionally or unintentionally. Intentionally inserting an impurity is called "doping." Thermal diffusion, doping during crystal growth, and ion implantation are methods of doping. Erbium (Er) and oxygen (O) are the two impurities used in this study. Note,

---

<sup>1</sup> Atomic energy levels are denoted as  $^{2S+1}L_J$ , where S is the spin angular momentum quantum number, L is the total electronic orbital angular momentum quantum number, and J is the total angular momentum quantum number. So,  $^4I_{15/2}$  means S=3/2, L=6, and J=15/2.



GaN:Er is shorthand notation for GaN implanted with Er. Similarly, GaN:Er+O is shorthand for GaN co-implanted with Er and O.

As mentioned in the previous paragraph, ion implantation is one way to dope a semiconductor. Ions are implanted by driving a beam of high energy ions into the material. Advantages include being able to use just about any ion and concentrations which exceed the thermal equilibrium concentration. In addition, unwanted contamination is limited and the concentration of dopants is controlled. However, the sample is damaged during the ion implantation. Results of damage include reducing minority carrier lifetime, reducing mobility, increasing the index of refraction of the material, and reducing the luminescence from the sample. Thus, the damage must be reduced or eliminated. Annealing, which is heating the sample to very high temperatures in a gas environment, repairs at least most of the damage. Furnace annealing is heating implanted materials in a furnace. If similar materials are positioned face-to-face during annealing, the process is called proximity annealing. Proximity annealing helps to prevent damage to the sample's surface which may result from the dissociation of atoms at the temperatures required for annealing.

As with a pure semiconductor, one must understand the behavior of the valence bands associated with an impurity to understand how the impurity affects the energy states of the host semiconductor. When a pentavalent (five valence electrons) impurity forms a molecule with the crystal lattice of the host semiconductor, energy states of the valence electrons associated with the impurity exist near, but slightly below, the minimum level of the CB, which is known as  $E_{CB}$  (see Fig. II-3).

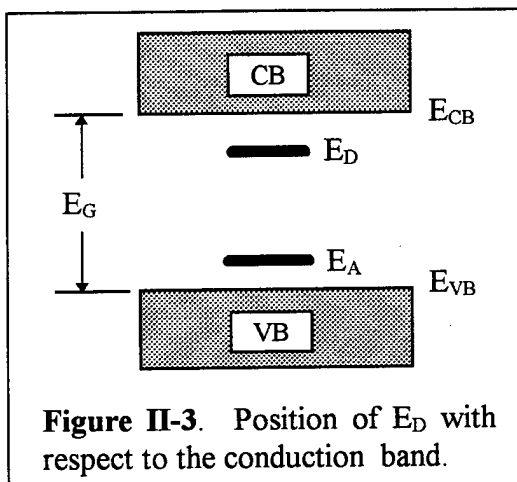


**Figure II-3.** Position of  $E_D$  with respect to the conduction band.

When this impurity forms a molecule with an atom in the crystal lattice, four of the valence electrons form covalent bonds with the four neighboring atoms and become part of the VB. The impurity is known as a donor since it gives the fifth electron to the host crystal. The extra electron can remain in the original energy state, denoted as  $E_D$ , or

absorb on the order of 0.01 eV and become part of the CB. While the electron remains at  $E_D$ , it is bound to the impurity atom. The lowest energy state of the CB is denoted as  $E_{CB}$ .

On the other hand, energy states of the valence electrons of a trivalent (three valence electrons) impurity reside slightly above the maximum energy state of the VB. As with the pentavalent impurity, the trivalent valence electrons join the VB and may obtain an electron from the crystal when they form covalent bonds with the host crystal, but this time a hole—not an electron—is left behind in the VB. The hole energy state, or unfilled energy state, is designated as  $E_A$  and can be seen in Fig. II-3. Note,  $E_A$  is on the order of 0.01 eV above the upper bound of the VB,  $E_{VB}$ . It is easy for an electron to occupy the hole, so this impurity is an acceptor. When an electron absorbs about 0.01 eV and jumps to  $E_A$ , it not only breaks a covalent bond and creates a hole, it becomes bound to the impurity atom.

Now, the question is how does Er affect the energy states of GaN? Once again, it is necessary to begin with the energy states of the valence electrons. When an impurity such as Er is implanted into a semiconductor, the impurity's energy states become meshed with the energy states of the host semiconductor. It is not known exactly how the energy

states of Er correlate to those of GaN. But, the electron configurations of both a free ion of Er and a triply-ionized Er ion in a host crystal are known and can be written as  $[Pd]4f^{12}5s^25p^66s^2$  and  $[Pd]4f^{11}5s^25p^6$ , respectively. Some of the energy states of erbium's 4f electrons are  $^4I_{11/2}$ ,  $^4I_{13/2}$ , and  $^4I_{15/2}$  (Silkowski, 1996:5-154). Note, the  $^4I_{15/2}$  state is the ground state,  $^4I_{13/2}$  is the first excited state, and  $^4I_{11/2}$  is the second excited state of trivalent erbium

Four possible radiative recombination processes result in luminescence and are shown in Fig. II-4. The first recombination process is a direct transition from the CB to the VB. In this process, known as a band-to-band transition, electrons can start slightly above or at the edge of the CB and they can end at the VB or in subbands of the VB.

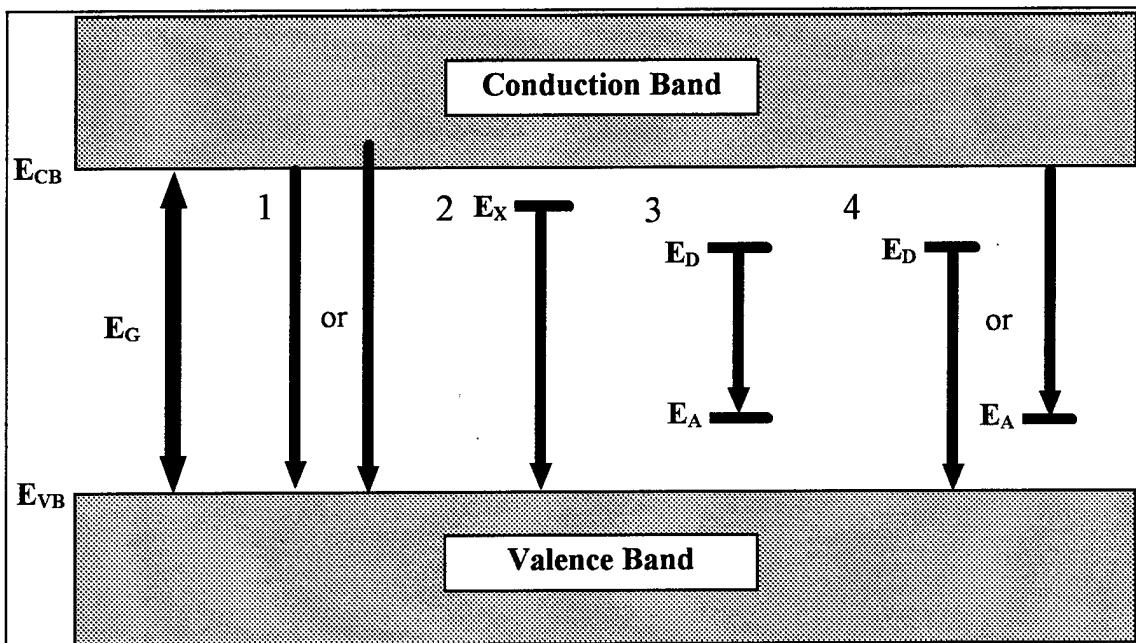


**Figure II-4.** Energy level diagram representing four different radiative recombination transitions. Transition 1 is a direct transition from the CB to the VB, 2 involves excitons, 3 is a donor-acceptor pair transition, and transition 4 is a free-to-bound transition.  $E_{CB}$  is the minimum energy state of CB while  $E_{VB}$  is the maximum energy state of the VB.  $E_G$  is the bandgap energy. Lastly,  $E_X$  is the energy state of an exciton,  $E_D$  is the energy state of a donor impurity, and  $E_A$  is the energy state of an acceptor impurity.

Ionization energy is the amount of energy needed to bind an electron to an impurity. When the temperature,  $T$ , is such that  $kT$  is greater than the ionization energy, some of the electrons break into the CB and remain as free carriers, which can then also de-excite from the CB to the VB. For a band-to-band transition in a direct bandgap semiconductor, luminescence,  $L$ , is given by the following relation

$$L(\nu) = B(h\nu - E_G)^{1/2}, \quad (2)$$

where  $\nu$  is the frequency of the photon,  $E_G$  is the bandgap energy, and  $B = \frac{2q^2 (m_r^*)^{3/2}}{nch^2 m_e^*}$

(Pankove, 1975:125). As usual,  $\frac{1}{m_r^*} = \frac{1}{m_e^*} + \frac{1}{m_h^*}$ ,  $m_e^*$  is the electron effective mass,  $m_h^*$  is the hole effective mass,  $m_r^*$  is their reduced mass,  $q$  is the magnitude of the electronic charge, and  $n$  is the index of refraction. The minimum energy that can be emitted is the bandgap energy.

In the second process of radiative recombination, excitons can recombine and produce luminescence in semiconductors. They can be associated with impurities. Electrons in the CB and holes in the VB generally move independently of each other. Nevertheless, at low temperatures, they can become bound. This bound state is called an exciton and it may be free or bound to an impurity. Several types of "bound" excitons exist. One type is when a free hole is attracted to a neutral donor, forming a positively charged excitonic ion. In this case, both the hole bound to the donor and its associated electron orbit the donor. Another type occurs when a free electron is attracted to a neutral acceptor. Free excitons can move through the crystal of the host semiconductor while bound excitons are tied to an impurity. Because the Coulombic attraction between

the electron and hole lessens the energy difference between the state occupied by the electron and the hole's energy state, the energy emitted when the electron recombines is less than the bandgap energy. As a result, the emission wavelength is slightly less than the wavelength associated with the bandgap energy. The ionization energy,  $E_x$ , of an exciton is given by the following equation:

$$E_x = -\frac{m_r^* q^4}{2h^2 \epsilon^2 n^2}, \quad (3)$$

where  $\frac{1}{m_r^*} = \frac{1}{m_e^*} + \frac{1}{m_h^*}$ ,  $m_e^*$  is the electron effective mass,  $m_h^*$  is the hole effective mass,  $m_r^*$  is their reduced mass,  $q$  is the magnitude of the electronic charge,  $h$  is Planck's constant,  $\epsilon$  is the dielectric constant of the semiconductor, and  $n$  is the quantum number of the exciton's state. If the exciton is free, then the energy of the emitted photon is

$$E_{Free} = h\nu = E_G - E_x. \quad (4)$$

On the other hand, if the exciton is bound, the emitted photon has an energy of

$$E_{Bound} = h\nu = E_G - E_x - E_B, \quad (5)$$

where  $E_B$  is the binding energy of the impurity (donor or acceptor) to which the exciton is bound (Pankove, 1975:120). Photoluminescence excitation studies indicate that the transition of a bound exciton is involved in the excitation of 4f-shell electrons in RE atoms (Kim, 1997:233).

The next process, process 3 in Fig. II-4, is sometimes referred to as a donor-acceptor (DA) pair transition, is a transition between a localized donor and a localized acceptor. The energy emitted,  $E_{Pair}$ , is

$$E_{\text{pair}} = h\nu = (E_G - E_D - E_A) + \frac{q^2}{\epsilon R}, \quad (6)$$

where  $E_D$  is the ionization energy of the donor,  $E_A$  is the ionization energy of the acceptor,  $\epsilon$  is the dielectric constant of the semiconductor, and  $R$  is distance between the donor and acceptor (Pankove, 1975:162). Note, the Coulombic force between the donor's electron and the acceptor's hole reduces the ionization energy because the donor and acceptor share the electron. When the donor and acceptor share an electron, it requires less energy to bind the electron to the impurities; therefore, the ionization energy is reduced. Transitions are more probable when the pairs are closer than when they are at a large  $R$ , so the intensity of the emissions should be greater when the pairs are at a small  $R$ . However, the number of possible DA pairings decreases with  $R$ . The net result is there is a minimum  $R$  at which the maximum intensity occurs. The distance between the donor and acceptor is a discrete quantity, but the spacings between emission peaks are very small [see Eqn. (6)]. On the other hand, the emission peaks overlap and form a broad spectrum when  $R$  is greater than 4 nm. Because of these phenomenon, only pair separations between 1 to 4 nm can be resolved in spectra from semiconductors (Pankove, 1975:143).

The final type of recombination process, called a free-to-bound transition, is a transition between 1) a donor and a hole in the VB or 2) an electron in the CB and an acceptor. These transitions emit photons of energy

$$h\nu = E_G - E_i, \quad (7)$$

where  $E_i$  is the ionization energy of the donor or an acceptor (Pankove, 1975:132-134).

All exciton, DA, and free-to-bound transitions can be phonon assisted, so it is necessary to understand transitions which involve phonons, too. The lattice of a

semiconductor normally vibrates due to kinetic energy when its temperature is greater than 0 K and dopants vibrate as the lattice of the host semiconductor vibrates. Phonons are quantized packets of the energy in lattice vibrations and may change energy states. Optical transitions may occur while the phonon changes energy states, possibly resulting in the emission or absorption of phonons. If only photons are emitted, a sharp line, called the zero phonon line, appears in the spectra at wavelengths corresponding to the energy of the transition. If, however, phonons are emitted with the photons, then smaller sidebands called phonon replicas appear near the sharp line.

Nonradiative recombination processes result in phonon emission.. There are three basic types of nonradiative recombination processes: multiphonon, Auger, and surface recombination. Two kinds of multiphonon recombination processes, which are nonradiative, exist. In the first type, an electron emits only a few phonons at a time as it drops from a very high excited state to lower states. The second type is the case in which an electron emits many phonons as it is captured nonradiatively. Auger recombination is the second main nonradiative recombination process. When an electron recombines with a hole by way of Auger recombination, the electron releases energy, which transfers to another electron or a hole via a phonon. Since Auger transitions are a result of three-body collisions of electrons and holes, the number of Auger transitions increases when temperature increases because the number of mobile electrons and holes increases with temperature. Lastly, note that Auger transitions can involve "hot" carriers. The third primary type of nonradiative recombination process is surface recombinations. When a lattice is perturbed or damaged, many "dangling bonds" form (Pankove, 1975:164). The

dangling bonds in a surface can trap impurities and create many deep and shallow energy levels, which can act as recombination centers.

How do electrons make transitions between energy states in GaN:Er and emit photons? Once an electron is excited to the CB, it can form an exciton bound to Er. When the bound exciton recombines, the resulting excess energy transfers via a phonon to the 4f energy states in Er and the excess energy dissipates as phonons. The photons around 1.54  $\mu\text{m}$  and 1.00  $\mu\text{m}$  are emitted when the excited 4f-electrons in Er make transitions from  $^4I_{13/2} \rightarrow ^4I_{15/2}$  and  $^4I_{11/2} \rightarrow ^4I_{15/2}$ , respectively. So, implanting Er into GaN results in more peaks in the luminescence spectra.

Electronic transitions of a free RE ion show up as sharp, well-resolved peaks in luminescence spectra. In a semiconductor implanted with a rare earth element, the outer 5s and 5p electrons of the RE element shield the inner 4f shell from the crystal field of the host crystal, so 4f shell electrons effectively do not interact with the host field. As a result, the 4f energy states and the transitions between the 4f energy states are not affected and continue to have sharp peaks in atomic spectra. The wavelengths associated with these peaks are constant as a function of the host and sample temperature. Because the peaks are sharp and constant with respect to the host and sample temperature, rare earths are ideal materials for use in LEDs and lasers.

#### **D. How Do Excitation Wavelength and Temperature Affect the Emissions?**

Both lasers and sample temperature can be used to excite electrons in a semiconductor to higher energy states and are discussed as excitation sources in this section.



Lasers can provide energy via photons to electrons in a semiconductor. The bandgap of GaN is 3.5 eV at 0 K. Above bandgap excitation is exciting the sample with more than 3.5 eV, which corresponds to wavelengths shorter than 354 nm since

$$E(\text{eV}) = \frac{hc}{\lambda} = \frac{1239.89}{\lambda(\text{nm})} \quad (8)$$

Recall E is excitation energy in eV, h is Planck's constant, c is the speed of light, and  $\lambda$  is the wavelength associated with the energy. Note, 354 nm is in the ultraviolet region of the radiation spectrum. This type of excitation can excite electrons directly to the CB. Similarly, below bandgap excitation uses energy less than 3.5 eV or wavelengths longer than 354 nm. In this case, electrons may be excited to impurity energy states within the bandgap.

Increasing sample temperature is another way of exciting electrons in a semiconductor. In general, electrical conductivity in a semiconductor increases exponentially with temperature since the number of electrons that are excited across the bandgap, N, is given by this relation

$$N \propto \exp\left[\frac{-E_G}{2kT}\right], \quad (9)$$

where  $E_G$  is the bandgap energy, k is Boltzmann's constant, and T is the temperature of the semiconductor. Note, GaN has a wide bandgap, so it is not as sensitive to temperature as are other semiconductors; however, the basic premise in Eqn. (9) still applies. A photon can excite an electron in the VB to the CB or a state in the bandgap. If the electron that is excited to a state below the CB receives an extra boost of energy and momentum from thermal excitation, it can then jump to the CB.

Increasing sample temperature not only increases the conductivity, it also changes the bandgap according to the following relation

$$E_G(T) = E_G(0) - \frac{\alpha T^2}{T + \beta}, \quad (10)$$

where  $E_G(0)$  is the energy gap at 0 K and  $\alpha$  and  $\beta$  are constants for a given semiconductor. The low temperature (0 K) bandgap of GaN is 3.5 eV, which is 354 nm while the 300 K bandgap is 3.39 eV, or 366 nm. The bandgap changes with temperature because it depends on the widths and splitting of the energy bands. The energy band boundaries and splitting, in turn, depend on the interatomic spacing, and the interatomic spacing increases as temperature increases. Consequently, the bandgap usually decreases as temperature increases.

Raising the sample temperature increases the conductivity of a semiconductor. However, radiative and nonradiative processes compete for the conduction electrons. As temperature increases, the number of phonons increases; thus, it is more likely that a decaying electron will collide with a phonon and lose its energy in a nonradiative process rather than make an optical transition. Fewer optical transitions mean fewer optical photons, which in turn, mean less luminescence.

In short, this chapter explains some background theory on the definition of semiconductors and energy bands; the relationship between the energy and wavelength of an emitted photon; ion implantation and annealing; and four recombination processes. Additionally, Chapter II discusses how impurities, excitation wavelength, and sample temperature affect the emissions from GaN. These concepts will enable the reader to better understand Chapters III and IV.

### III. Samples, Procedures, and Equipment

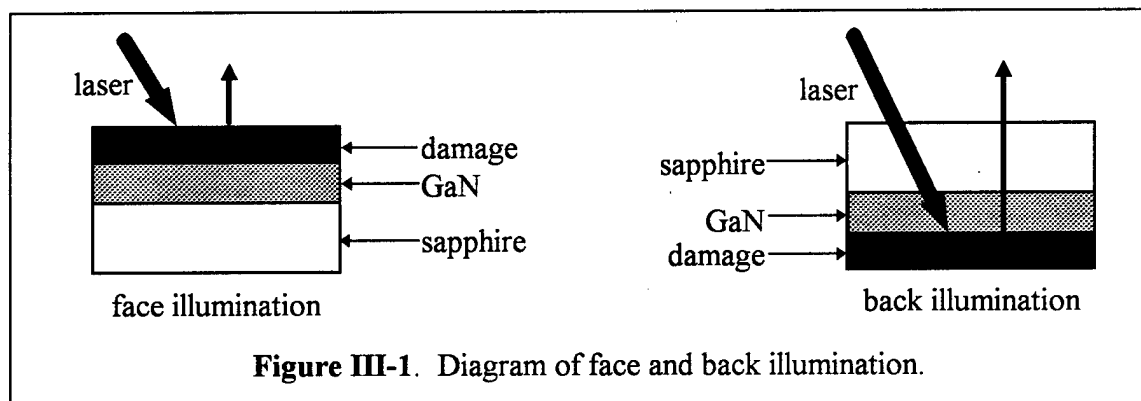
This chapter describes the sample preparation in Part A; explains the procedures used to obtain photoluminescence (PL) spectra, Part B; and lists the equipment used in the experiment in Part C.

#### A. Samples

The first paragraph in Part A discusses how the samples were grown, implanted, and annealed and the second paragraph explains how the samples are mounted. The three samples used in this experiment are also used in Silkowski's work and are prepared as described in the following sentences. One wafer of as-grown gallium nitride (GaN) from Honeywell is used to prepare all three samples used in this experiment. The GaN wafer was grown by metal-organic chemical vapor deposition (MOCVD) on c-plane sapphire and then cut into three pieces. One of the pieces is designated as sample A. Erbium (Er) and/or oxygen (O) ions were then implanted into the remaining two pieces of GaN. Er was implanted into both the second (sample B) and third pieces of GaN at 1150 keV at a dose of  $5 \times 10^{13} \text{ cm}^{-2}$  and a peak concentration of  $4.9 \times 10^{18} \text{ cm}^{-3}$ . Then, sample C was further prepared by implanting oxygen (O) into the third piece with 135 keV at a dose of  $5 \times 10^{14} \text{ cm}^{-2}$  and a peak concentration of  $2.8 \times 10^{19} \text{ cm}^{-3}$ . The implantation energies are such that the peak concentrations of Er and O occur at about the same depth in the GaN:Er+O sample. The Er sample (sample B) was annealed with the proximity cap method in an ammonia ( $\text{NH}_3$ ) environment for 90 minutes at 1000 °C while the Er+O sample (sample C) was annealed under identical conditions, but at 800 °C. These two annealing temperatures are used because GaN:Er and GaN:Er+O have different optimum

annealing temperatures, which are 1000 °C and 800 °C, respectively (Silkowski, 1996:5-176). One can assume these "samples have a high dislocation and defect densities, significant quantities of unintentional dopants," and are not necessarily perfect crystals (Silkowski, 1996:3-15).

The samples are mounted to a cold finger by either gluing them with rubber cement or using black wax to attach them. When the laser beam illuminates the samples during the experiments, the rubber cement emits visible photons, so black wax must be used when scanning the samples in the visible region. In addition, the samples are mounted such that the GaN:Er sample (sample B) is face-illuminated, while the GaN:Er+O sample (sample C) is back-illuminated due to severe damage on the face. See Fig. III-1 for a graphic explanation of face and back illumination.



If the sample is face-illuminated, then the sapphire side is directly attached to the mount while a back-illuminated sample is attached with the GaN film closest to the mount.

## B. Procedures

Once the samples were prepared, two sets of experiments are conducted on the samples. The first set of experiments measures the PL intensity from GaN near the bandedge. Since the bandgap of GaN is 3.5 eV (or 354 nm), the GaN sample (sample A)

is scanned from 350 to 850 nm. Furthermore, the range of the PMT is limited to above 350 nm, so the sample cannot be scanned below 350 nm. The excitation wavelength is the 333.6-363.8 nm multiline and each sample is at 2 K. In a multiline, the laser lases at several different wavelengths simultaneously over a range of wavelengths.

In the second set of experiments, the effects of excitation wavelength and sample temperature on Er emissions are studied while scanning the two doped samples (B and C) from 1515-1575 nm and 970-1070 nm. The photons emitted at these wavelengths are targeted because previous work shows Er transitions from the  $^4I_{13/2}$  manifold to the ground state around 1500-1620 nm and similar transitions from the  $^4I_{11/2}$  manifold to the ground state at about 970-1050 nm. In this experiment, the focus is on the 1540-nm peak so the scanning range is smaller than in previous work. Initially, the PL intensity from each sample is measured as a function of excitation wavelength. In order to study the effects of excitation wavelength on the Er luminescence and the optimum excitation wavelength, samples B and C are illuminated with multiple wavelengths from 275.4-305.5 and 333.6-363.8 nm and single wavelengths of 488.0 and 514.5 nm. Laser power is kept constant at 400 mW for all wavelengths and sample temperature is maintained at 2 K. Once the optimum excitation wavelength for each of the doped samples is known, the sample temperature is varied from 2-150 K in increments of 25 K while exciting the sample at its optimum excitation wavelength.

The method of collecting the PL spectra is described below and is depicted in Fig. III-2. An Argon (Ar)-ion laser produces a laser beam. Two prisms then steer the laser beam through a chopper and onto the samples. Next, two lenses collect and focus the luminescence from the samples into the spectrometer. The grating in the spectrometer

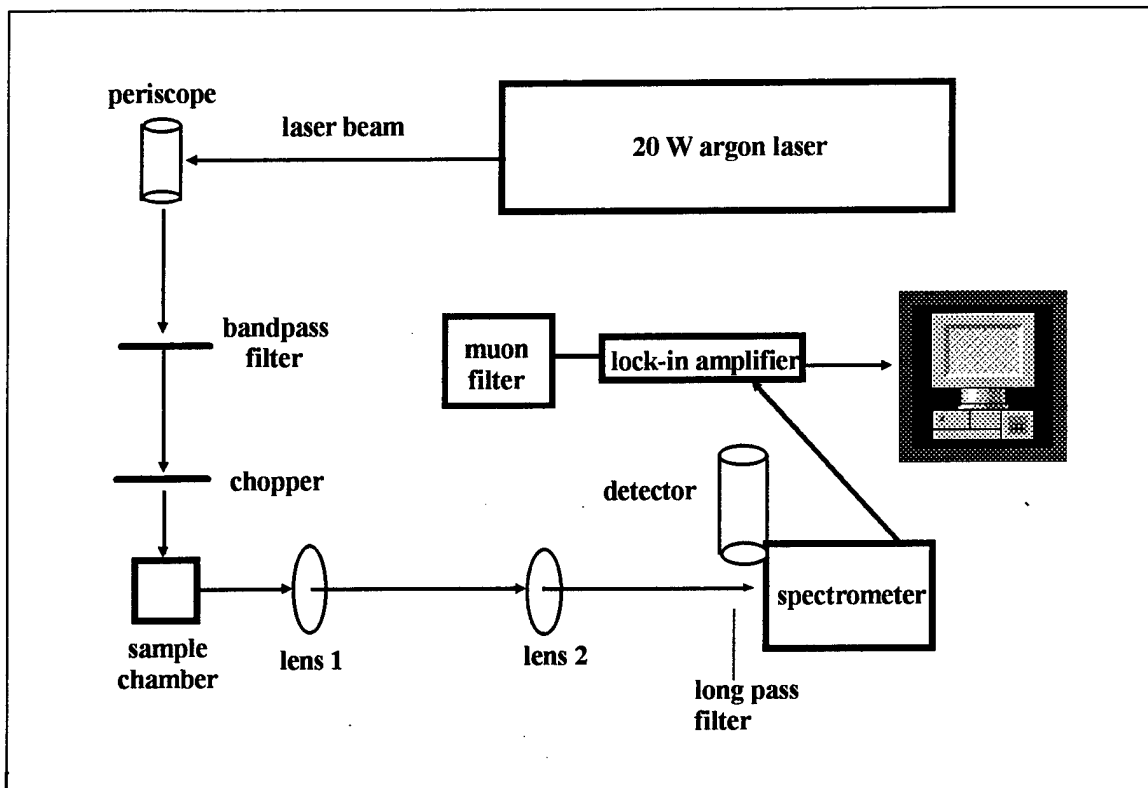


**Figure III-2.** Setup used to measure the PL intensity from GaN, GaN:Er, and GaN:Er+O. A PMT detected luminescence from GaN and the Ge detector was used for the other two samples.

disperses the light to either the photomultiplier tube (PMT) or the germanium (Ge) detector. The PMT converts the PL signal into current, but the Ge detector converts the luminescence from the spectrometer into an output voltage. The current from the PMT passes directly to the computer, which interprets, plots, and stores each luminescence spectrum. However, the voltage from the Ge detector is fed into a lock-in amplifier, magnified, and then sent to the computer. More information about the purpose of each of the above devices is provided in the following section.

### C. Equipment

The equipment can be divided into four subsystems: excitation source, pressure control, temperature control, and data acquisition. Table III-1 (p III-7) lists the

manufacturers and model numbers of the equipment used to study PL from both undoped and doped GaN. Table III-2 (p III-8) lists the equipment and the settings used during the experiments.

As mentioned previously, the excitation source is an Ar-ion laser. Samples can be excited with multiple wavelengths from 275.4-305.5 and 333.6-363.8 nm and single wavelengths of 488.0 and 514.5 nm. The laser power is maintained at 400 mW for all wavelengths. As long as the laser beam is not high power (or tightly focused), then the damage from the laser is minimal.

The second subsystem controls the pressure of the sample chamber and vacuum jacket of the dewar. This system consists of a roughing pump and a turbomolecular pump. The mechanical roughing pump reduces the pressure of the sample chamber from 760 mm Hg (atmospheric pressure) to below 50  $\mu\text{m}$  Hg. Then, the turbomolecular pump decreases pressure in the vacuum jacket to less than 0.1  $\mu\text{m}$  of Hg. The purpose of the vacuum jacket is to isolate the helium (He) reservoir from the nitrogen ( $\text{N}_2$ ) reservoir and the  $\text{N}_2$  reservoir from the environment.

Another subsystem comprising a cryogenic dewar and a temperature controller regulates the temperature of the samples. The cryogenic dewar has a liquid He reservoir surrounded by a liquid  $\text{N}_2$  reservoir. The liquid  $\text{N}_2$  chamber pre-cools the liquid He chamber to prevent the liquid He from evaporating quickly. The operator adjusts the amount of liquid by opening and closing a needle valve which allows more or less liquid He to flow from the reservoir into the sample chamber. By adjusting the amount of liquid He in the depressurized sample chamber, samples can be cooled to 1.40 K. The second part, a temperature controller, heats the sample mount and displays the temperature of the

samples. It is accurate to within 0.1 K from 1.40 to 100 K and within 1.0 K from 100 to 300 K. Data does not exist for temperatures greater than 150 K due to equipment failure.

The last subsystem for PL data is the data acquisition subsystem, which consists of the chopper, lenses, filters, spectrometer, detectors, muon filter, lock-in amplifier, and computer. Note, the chopper, muon filter, and lock-in amplifier are used with the Ge detector, not the PMT. The purpose of the chopper is to transform the continuous wave laser beam into a frequency-modulated square wave. The lenses focus the luminescence onto the spectrometer entrance slit. Since measuring laser light is undesirable, using the long pass filter and carefully positioning the samples is necessary to prevent laser light from passing into the spectrometer. The slits on both the entrance and exit ports of the spectrometer are set at 100  $\mu\text{m}$  in order to achieve very good resolution. The spectra are calibrated with a krypton lamp, but are not corrected for the spectral response of the grating or detectors. Even though the PMT has a great signal-to-noise ratio, it can detect only visible and ultraviolet transitions. Consequently, the Ge detector must be used while scanning the samples in the infrared. The Ge detector does not have a good signal-to-noise ratio; and as a result, the output signal must be amplified. The lock-in amplifier detects only the signal that is at the chopper frequency and then amplifies that signal. The settings on the muon filter and lock-in amplifier optimize the signal-to-noise ratio. Once the signal reaches the computer, Microcal's Spex software is used to plot the spectrum. Wavelength values are reported to the nearest 1 nm, in general, because of the inaccuracies in reading them from the plots.



**Table III-1. List of Equipment Used to Collect Photoluminescence**

Item	Manufacturer	Model Number/Specifications	Serial Number
20 W Argon ion laser	Spectra Physics	Beamlok™ 2080/85-20S 400-20/A	188
mechanical oil pump	The Welch Scientific Company	1397	14327
mechanical roughing pump	Alcatel	1091045400	
turbomolecular pump	Alcatel	cfv100	2012A
cryogenic dewar	Janis Research Co., Inc.	10DT	4916R
temperature control	LakeShore	8054 W60	
prisms	Oriel	46160	
power meter	Coherent	200 Series	BM56
chopper	Stanford Research Systems, Inc.	SR540	
lens 1	Newport Corporation	BC7 BCX, uncoated focal length = 100 mm	
lens 2	"	BC7 BCX, uncoated focal length = 300 mm	
long pass filter		1000	
spectrometer	Spex	750 M 600 gr/mm resolution = 0.01 nm	0123
spectrometer control	Spex	232-MSD	
germanium detector	North Coast Scientific Corp.	EO-817L cooled with liquid N <sub>2</sub> spectral response = 0.8- 1.7 μm	
photomultiplier tube	Products for Research, Inc.	TE176TSRF cooled with liquid N <sub>2</sub>	19753-94
muon filter	North Coast Scientific Corp.	829B	
bias supply for Ge detector	"	823A	
lock-in amplifier	Stanford Research Systems	SR830 DSP	
computer	Spex	PC486	
plotting programs	Spex Microcal Software, Inc.	dM3000 Origin™	

**Table III-2. Equipment Settings Used to Collect Photoluminescence**

Item	Setting
20 W Argon-ion laser wavelengths	275.4-305.5, 333.6-363.8, 488.0, 514.5 nm
temperature control	2-150 K
power meter	400 mW
chopper 90	92 Hz
spectrometer	350-850 and 970-1650 nm 600 gr/mm
muon filter	
gain	150
hold time	370 msec
integrate time	1 sec
bias supply for Ge detector	200 V
lock-in amplifier	
time constant	300 msec, 12 dB, Sync <200 Hz
sensitivity	5 mV

This chapter describes the apparatus used to measure the PL intensity from GaN doped with only Er and from GaN doped with both Er and O. The next chapter discusses the results of the experiment.

## Chapter IV. Results and Discussion

Luminescence intensity is important because an engineer needs to know how much and at what wavelength will the intensity occur in order to design a device that the United States Air Force can use. It is necessary to understand undoped GaN as a baseline before studying the effects of excitation wavelength and sample temperature on doped GaN in order to determine how the impurities affect the host semiconductor. This study measured PL spectra from GaN, GaN implanted with Er alone (GaN:Er), and GaN co-implanted with oxygen (GaN:Er+O). The results are presented in five parts. Part A describes the PL spectra of as-grown GaN. Part B discusses the PL spectra of doped GaN. Parts C and D present the effects of changing the excitation wavelength and sample temperature, respectively, and are divided into two sections: Er alone and Er co-doped with O. Finally, Part E compares the photoluminescence (PL) intensity from GaN: Er and GaN:Er+O as a function of excitation wavelength and sample temperature. Comparisons amongst the spectra were made based on the integrated intensity, or area under the curve, of the PL signal.

### A. Photoluminescence Spectra of As-Grown GaN

Part A discusses the spectrum from as-grown GaN (sample A). Despite all of the information about GaN that exists, this report of the PL emissions from GaN that was excited with 275.4-305.5 nm laser line and scanned from 3.54-1.46 eV (350-850 nm). The spectra are shown in Figs. IV-1 and IV-2. The goal was to find evidence of the exciton, DA, one longitudinal optical (LO) and two LO transitions. Tables IV-1 and IV-2 compare the peak locations of exciton transitions from previous work to the values

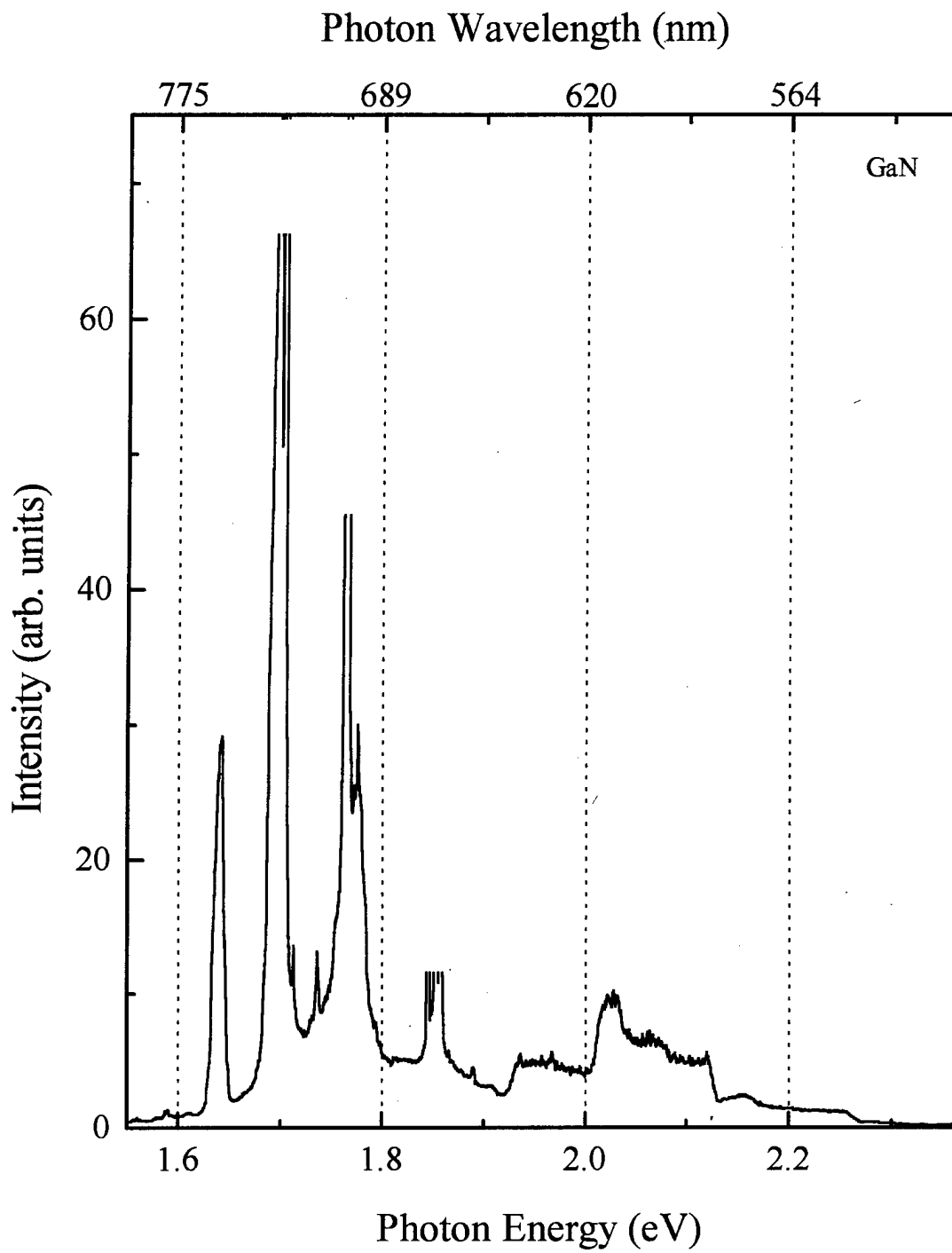


**Figure IV-1.** PMT spectrum of as-grown GaN excited with the 333.6-363.8 nm multiline and sample temperature of 2 K.

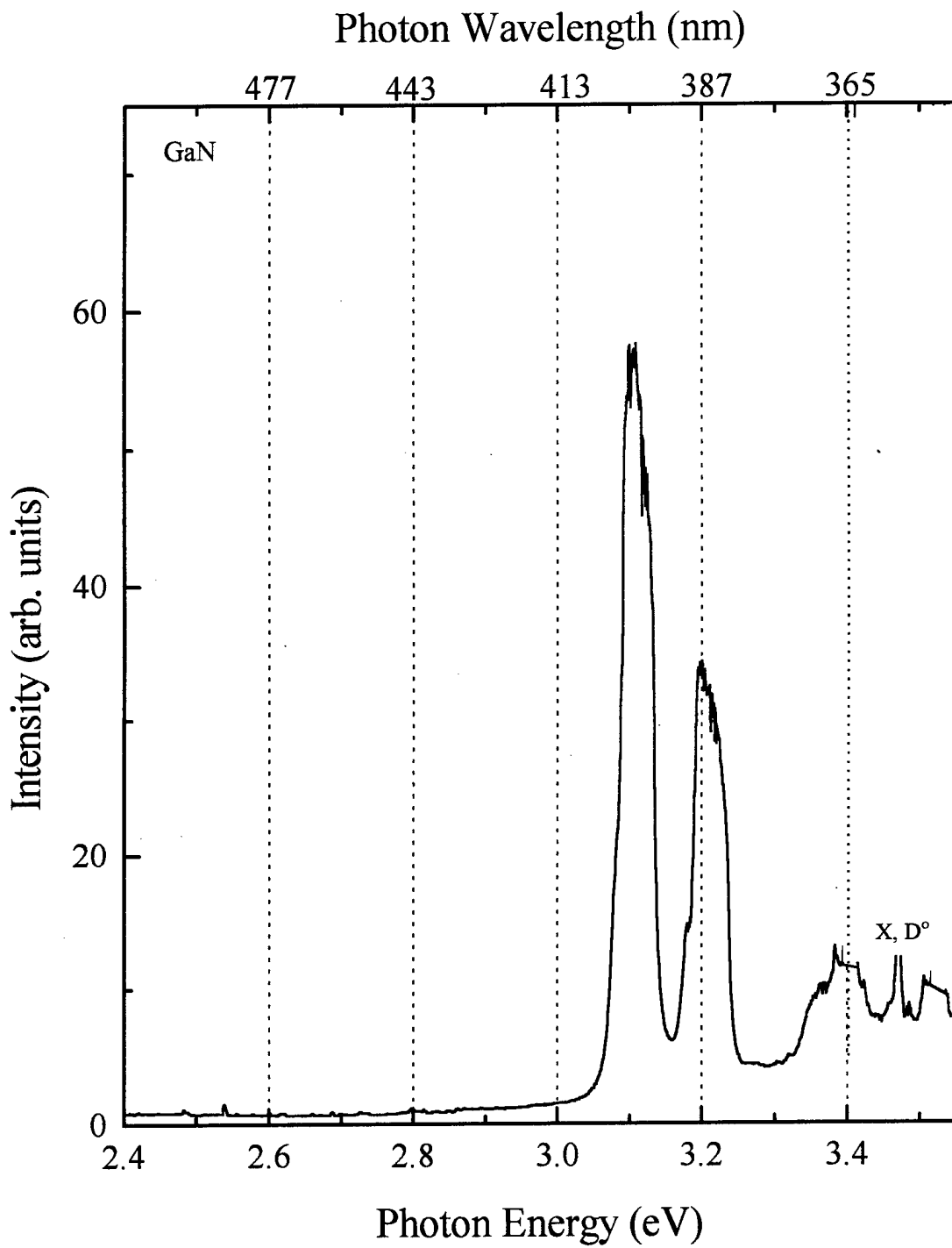


**Figure IV-2.** PL spectrum of as-grown GaN excited with the 333.6-363.8 nm multiline and sample temperature of 2 K. X represents the exciton and  $D^{\circ}$  is the neutral donor.

obtained in this work. Even though the samples in the Tables were grown with different techniques, the experimental values are similar. Silkowski and Everitt used the same sample. Note, X indicates exciton, ND represents neutral donor, and NA means neutral acceptor. The growth mechanisms listed in the tables include vapor phase epitaxy (VPE), needle, powder, metal-organic vapor phase epitaxy (MOVPE), and metal-organic chemical vapor deposition (MOCVD).

**Table IV-1. Experimental Values of X-ND Transition**

Author	Growth	X Bound to ND (eV)	X Bound to ND (nm)
Dingle	VPE	3.467	357.6
Matsumoto	Needle	3.4716	357.2
Largerstedt & Monemar	VPE	3.469	357.4
Ogino & Aoki	Powder	3.472	357.1
Ogino & Aoki	Powder	3.4719	357.1
Amano	MOVPE	3.49	355.3
Ilegems & Dingle	VPE	3.465	357.8
Vavilov	VPE	3.472	357.1
Marasina	VPE	3.4685	357.5
Shan	VPE	3.479	356.4
Silkowski	MOCVD	3.48	356
Everitt	MOCVD	3.47	357

**Table IV-2. Experimental Values of X-NA Transition**

Author	Growth	X Bound to NA (eV)	X Bound to NA (nm)
Dingle	VPE	3.455	358.9
Ilegems & Dingle	VPE	3.455	358.9
Pikhtin	Bulk	3.455	358.9
Vavilov	VPE	3.455	358.9
Silkowski	MOCVD	--	--
Everitt	MOCVD	3.457?	358.7

The transition of an exciton bound to a neutral donor occurred at 3.47 eV (357 nm) for the sample used in this work, which agreed with previous values listed in Table IV-2. Furthermore, this author observed a small shoulder at 3.457 eV (358.7 nm) on the peak

corresponding to the transition of the exciton bound to a neutral donor that could be evidence of the transition of the exciton bound to a neutral acceptor.

Table IV-3 lists experimental values of the DA as well as the one LO and two LO phonon replica transitions.

**Table IV-3. Experimental Values of the DA, 1 LO, and 2 LO Transitions**

Author	Temperature (K)	DA (eV & nm)	1 LO (eV & nm)	2 LO (eV & nm)
Grimeiss & Monemar	4.2	3.27 eV 379.2 nm	3.18 eV 389.9 nm	3.09 eV 401.3 nm
Dingle & Ilegems	1.6	3.2571 eV 380.7 nm	3.1672 eV 391.5 nm	3.0768 eV 403.0 nm
Cunningham	77	3.27 eV 379.2 nm	3.18 eV 389.9 nm	3.09 eV 401.3 nm
Ilegems	4.2	3.268 eV 379.4 nm	--	--
Matsumoto & Aoki	4.2	3.264 eV 379.9 nm	3.174 eV 390.6 nm	3.08 eV 402.6 nm
Matsumoto & Aoki	4.2	3.27 eV 379.2 nm	3.18 eV 389.9 nm	
Matsumoto	4.2	3.268 eV 379.4 nm	3.187 eV 389.0 nm	3.097 eV 400.4 nm
Lagerstedt & Monemar	4.2	3.263 eV 380.0 nm	--	--
Dai	10	3.311 eV 374.5 nm	--	--
Silkowski	2	3.28 eV 378 nm	3.18 eV 390 nm	3.06 eV 405 nm
Everitt	2	--	--	--

Expected values of the DA, one LO, and two LO transitions are 3.27, 3.18, and 3.09 eV (379, 390, and 401 nm) (Silkowski, 1996:5-2). None of these transitions were observed. However, strong peaks at 3.1 and 3.2 eV (400 and 387 nm) were observed, as shown in Figs IV-1 and IV-2. The origins of these peaks are unknown at present.

## **B. Photoluminescence Spectra of Doped GaN**

This part first identifies peaks in the PL spectra of implanted GaN. The first step was to record a spectrum from Silkowski's Er-doped GaN sample under conditions similar

to those that Silkowski used. Then, the peak positions in each of the spectra were labeled consistently with Silkowski's labels. A detailed comparison of the 1.54  $\mu\text{m}$  emission spectrum is in Appendix A. See Fig. IV-3 to see how the peaks were labeled.

The second step was to collect spectra showing the peak locations of the  $^4\text{I}_{13/2} \rightarrow ^4\text{I}_{15/2}$  and  $^4\text{I}_{11/2} \rightarrow ^4\text{I}_{15/2}$  transitions for both Er-doped and co-doped GaN. Both samples were scanned from 1515-1575 and 970-1070 nm and were excited with the 333.6-363.8 nm multiline while at 2 K. The photons were emitted at the same wavelength for both GaN:Er (sample B) and GaN:Er+O (sample C). The peaks corresponding to transitions between the  $^4\text{I}_{13/2} \rightarrow ^4\text{I}_{15/2}$  and  $^4\text{I}_{11/2} \rightarrow ^4\text{I}_{15/2}$  energy states are listed in Appendix B. The most important result in this section is that Er transitions occurred at 0.8104 eV (1.54  $\mu\text{m}$ ) and 1.251 eV (0.991  $\mu\text{m}$ ) for the samples used in this work, which is consistent with Silkowski's work.

### C. Effects of Changing the Excitation Wavelength of Doped GaN

Part C investigates the intensity of PL emissions from GaN:Er and GaN:Er+O at different excitation wavelengths in order to learn about the excitation mechanism of RE ions. An Ar-ion laser excited the samples at 2 K with 275.4-305.5 and 333.6-363.8 nm multiline as well as 514.5 and 488.0 nm lines. More information about the samples and equipment is in Chapter III. Both samples were scanned from 1515 to 1575 nm and from 970 to 1070 nm to observe the  $^4\text{I}_{13/2} \rightarrow ^4\text{I}_{15/2}$  transitions at about 1.54  $\mu\text{m}$  and the  $^4\text{I}_{11/2} \rightarrow ^4\text{I}_{15/2}$  transitions around 0.991  $\mu\text{m}$ . Only peaks A-H (see Fig. IV-4) and 5-7, 10, and 17-18 (see Fig. IV-5) were noted because they were some of the most intense transitions in their respective spectrum.



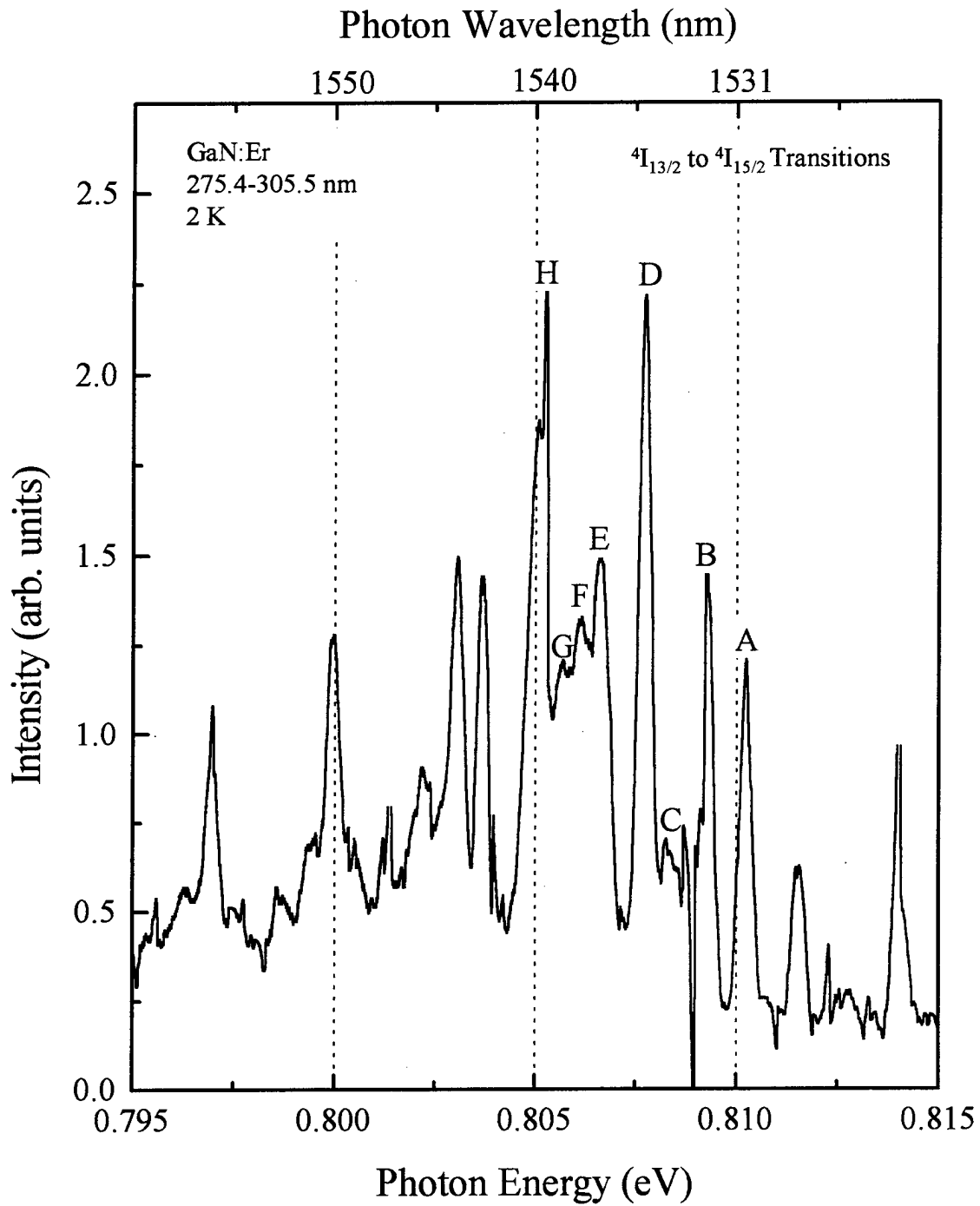


**Figure IV-3.** A PL spectrum from GaN:Er, excited by 275.4-305.5 nm and was scanned over a spectral range of 1525-1560 nm. The laser power was 400 mW.

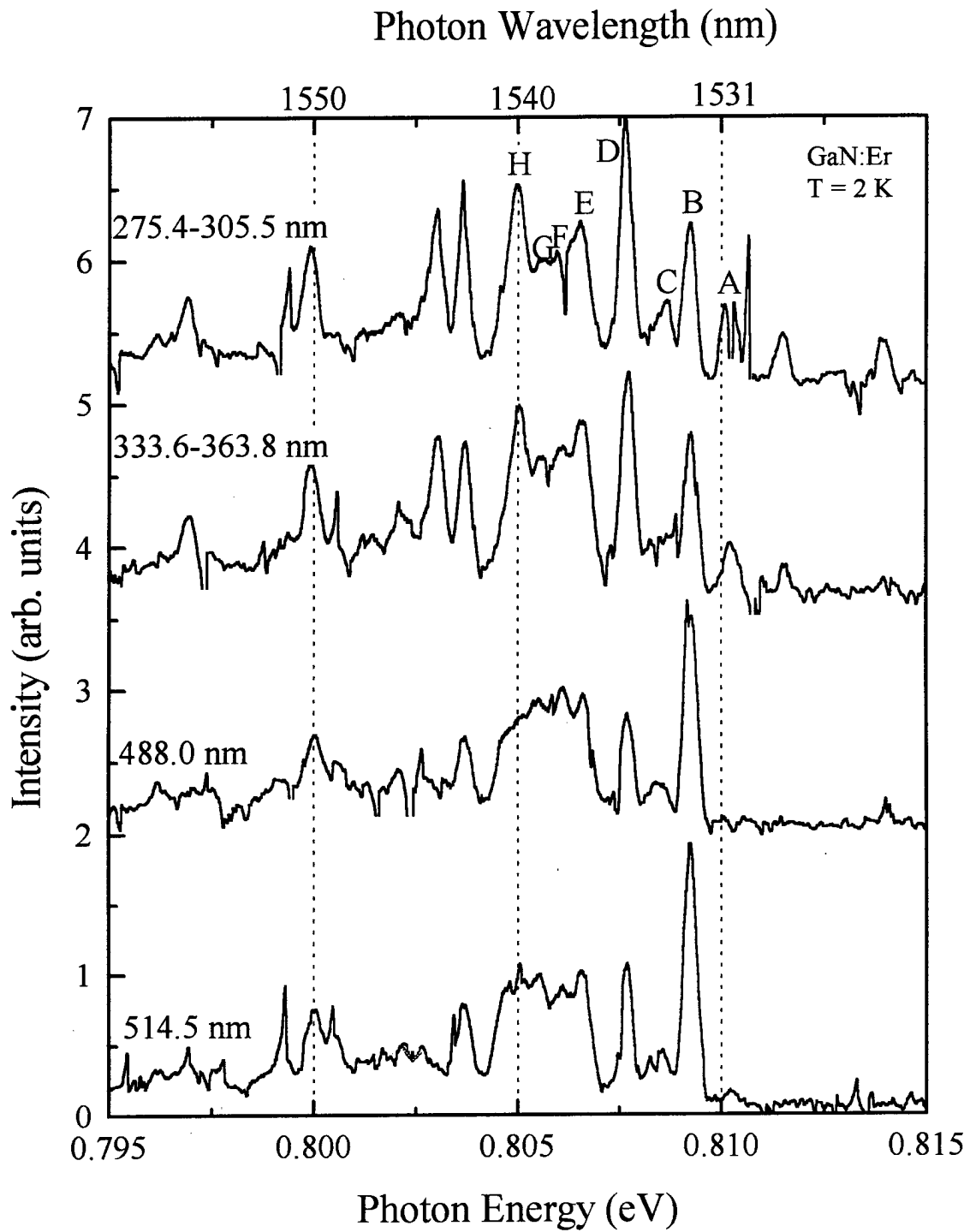


**Figure IV-4.** PL spectra of GaN:Er as a function of excitation wavelength. Sample temperature is 2 K. Laser power is 400 mW.

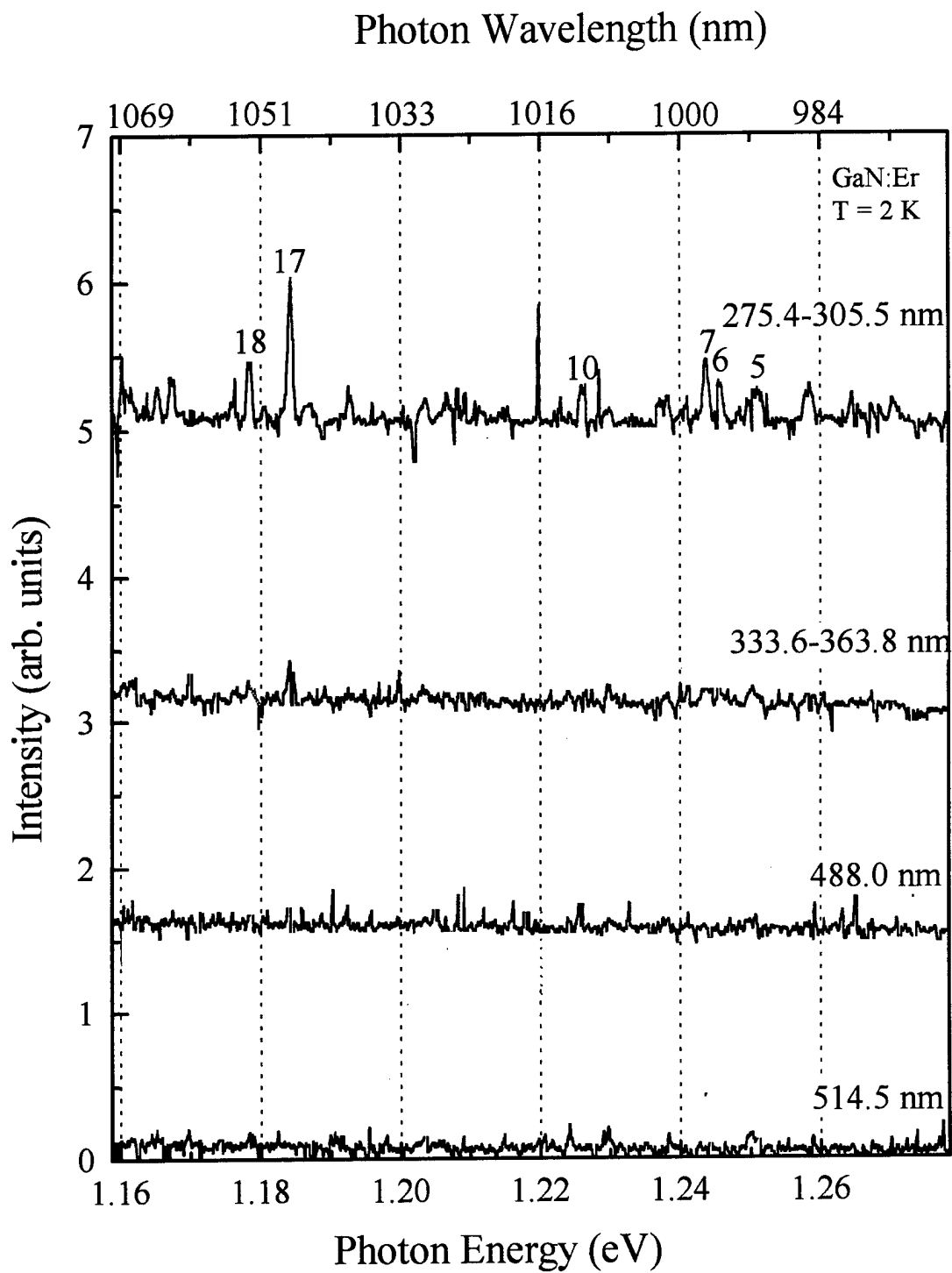


**Figure IV-5.** PL spectra of GaN:Er as a function of excitation wavelength. Sample temperature is 2 K. Laser power is 400 mW.

## 1. GaN Doped with Erbium

Changing the excitation wavelength influenced the PL intensity for transitions from both manifolds. The spectra showing the effects of excitation wavelength on PL emissions from GaN:Er are depicted in Figs. IV-4 and IV-5. The integrated intensity of PL intensity emitted around 1.54  $\mu\text{m}$  from GaN:Er was about the same for both UV and the 514.5-nm excitation lines, but the 488.0 nm wavelength induced a PL signal whose integrated intensity was slightly smaller. Note that the B peak decreased and the H peaks increased as excitation wavelength decreased. This different behavior implies that they originate from different luminescence centers. At the same time, GaN:Er emitted significant peaks around 0.991  $\mu\text{m}$  only when excited by the 275.5-305.5 nm wavelengths. Peak locations of transitions from both the  $^4I_{13/2}$  and  $^4I_{15/2}$  manifolds were constant.

## 2. GaN Doped with Erbium and Oxygen

The spectra taken as a function of excitation wavelength from GaN:Er+O are in Figs. IV-6 and IV-7. Unlike GaN:Er, the PL integrated intensity emitted from GaN:Er+O at 1.54  $\mu\text{m}$  and induced by the 333.6-363.8 nm multiline was slightly higher than the integrated intensity when the 275.4-305.5 nm multiline was used. Similar to emissions from GaN:Er, the 488.0 nm laser line excited about the same PL intensity around 1.54  $\mu\text{m}$  from sample C as the 514.5 nm line, but drastically less than those of the above bandgap excitation lines. Peaks were stronger when visible wavelengths excited GaN:Er+O. In the 0.991- $\mu\text{m}$  spectrum, sample C emitted strongly when it was illuminated with either of the above bandgap excitation wavelengths; and as with sample B, neither of the below bandgap wavelengths resulted in significant PL intensity. It was interesting to note peak

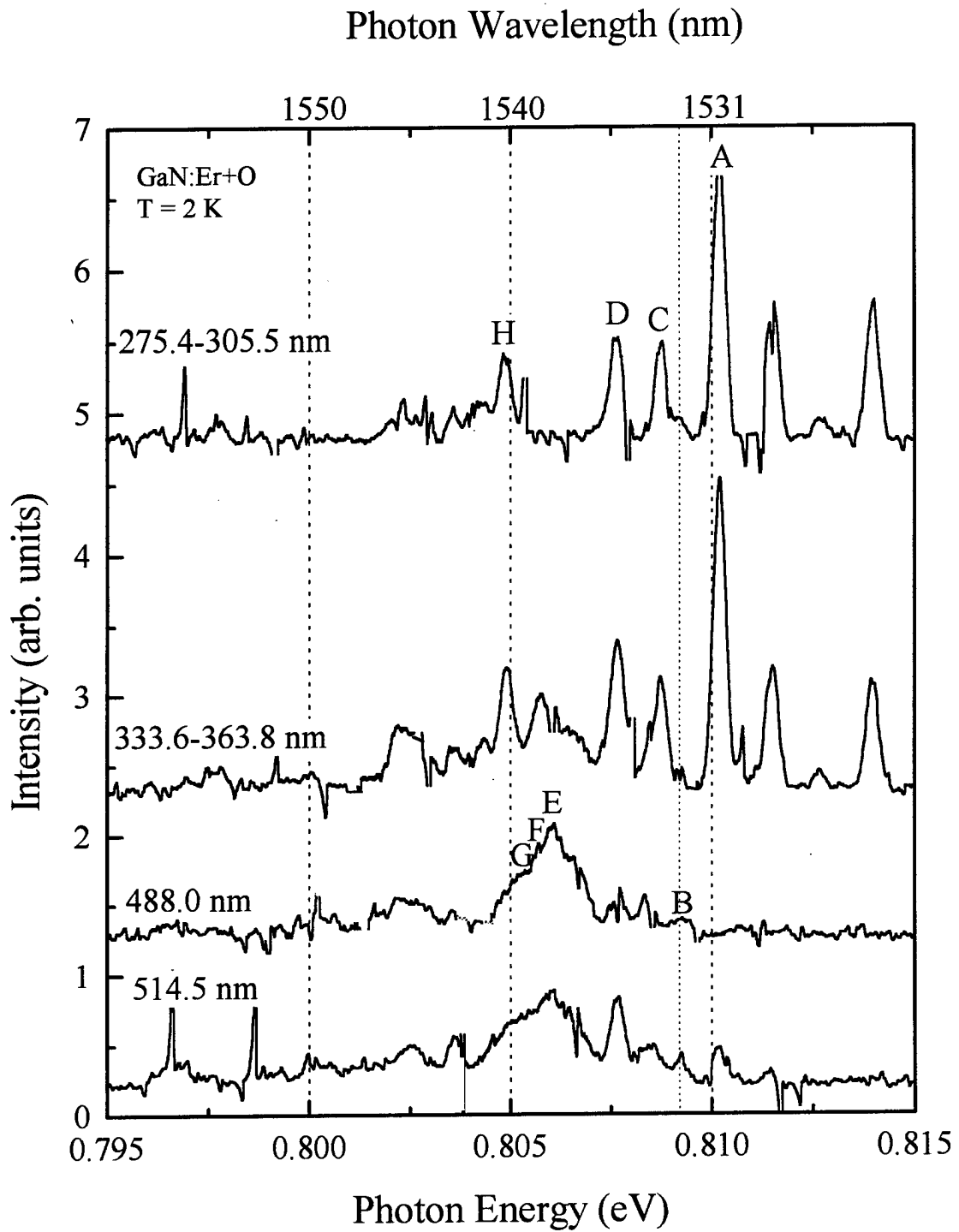


**Figure IV-6.** PL spectra of GaN:Er+O as a function of excitation wavelength. Sample temperature is 2 K. Laser power is 400 mW.

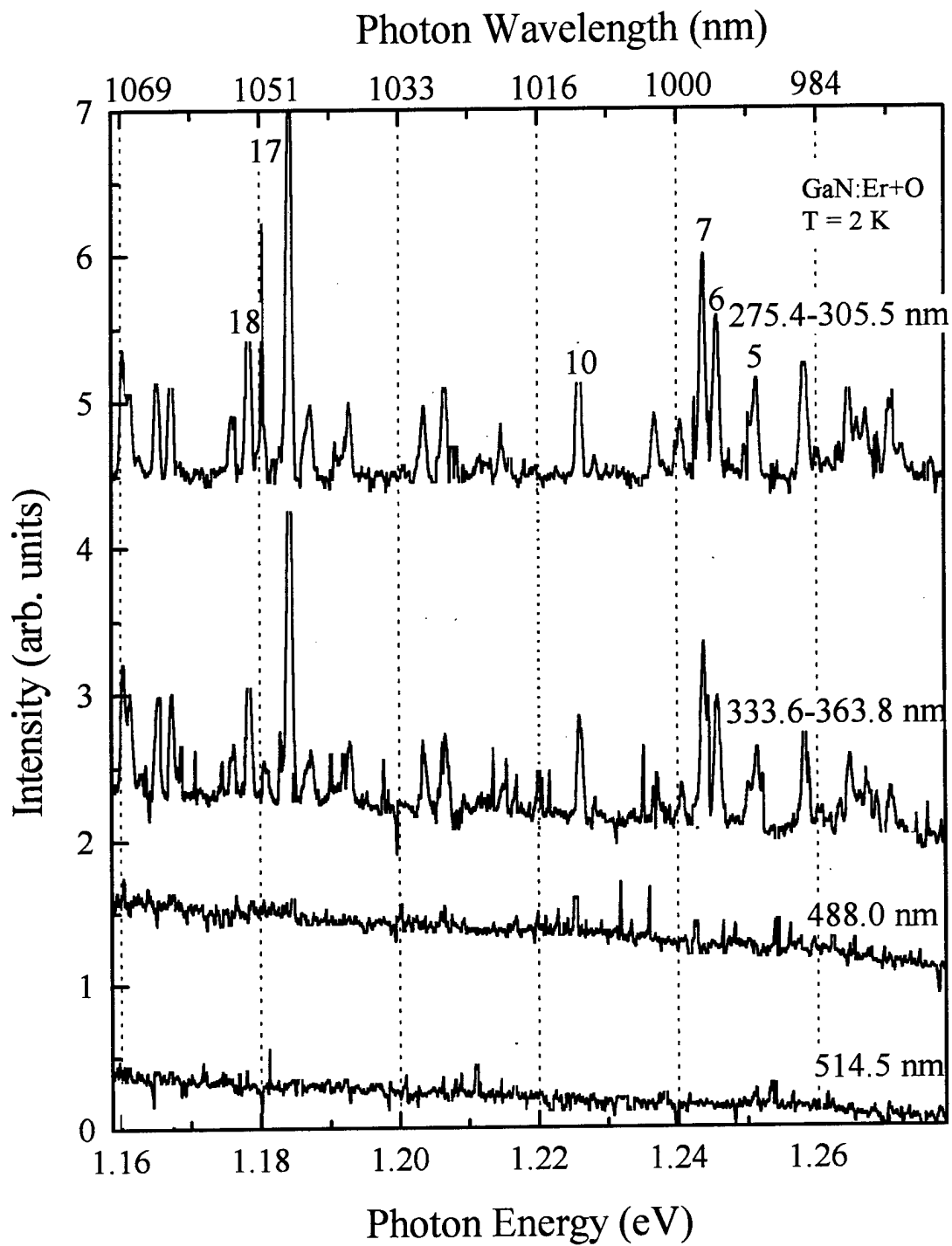


**Figure IV-7.** PL spectra of GaN:Er+O as a function of excitation wavelength. Sample temperature is 2 K. Laser power is 400 mW.

17 is the dominant peak in the 0.991  $\mu\text{m}$  spectrum group. As with GaN:Er, the locations of emissions from sample C were constant as the excitation wavelength changed.

#### **D. Effects of Changing the Sample Temperature of Doped GaN**

Since research efforts are directed at trying to find materials for Er-emission LEDs and laser diodes (LDs) that operate at room temperature, this work studied the PL from samples B and C as a function of sample temperature. This part, Part D, discusses the results of that study. Temperature was increased from 2 to 150 K in increments of 25 K. Results are presented for all of the data, but only the spectra taken 2, 75, and 150 K are discussed because the other temperatures follow the same trend. The samples were excited at their optimal wavelength; that is, GaN:Er was excited by the 275.5-305.5 nm multiline and the 333.6-363.8 nm multiline excited the co-doped sample.

##### 1. GaN Doped with Erbium

The effect of increasing sample temperature on the emissions from GaN:Er is shown in Figs. IV-8 to IV-9. The integrated intensity of the PL emissions from sample B decreased as temperature increased due to a smaller number of excitons bound to Er; yet, the emissions did not decrease by much. The integrated intensity of transitions which emit photons around 1.54  $\mu\text{m}$  decreased by 38% while the emissions around 0.991  $\mu\text{m}$  decreased by only 22%! In fact, peaks A, C, D, H and peaks 5-7, 10, and 17-18 remained strong at 150 K.

##### 2. GaN Doped with Erbium and Oxygen

Sample temperature had a more interesting effect on the GaN:Er+O sample than on the GaN:Er sample. The PL spectra are depicted in Figs. IV-10 and IV-11. As with GaN:Er, most of the peaks in the 1.54  $\mu\text{m}$  spectrum decreased as temperature increased

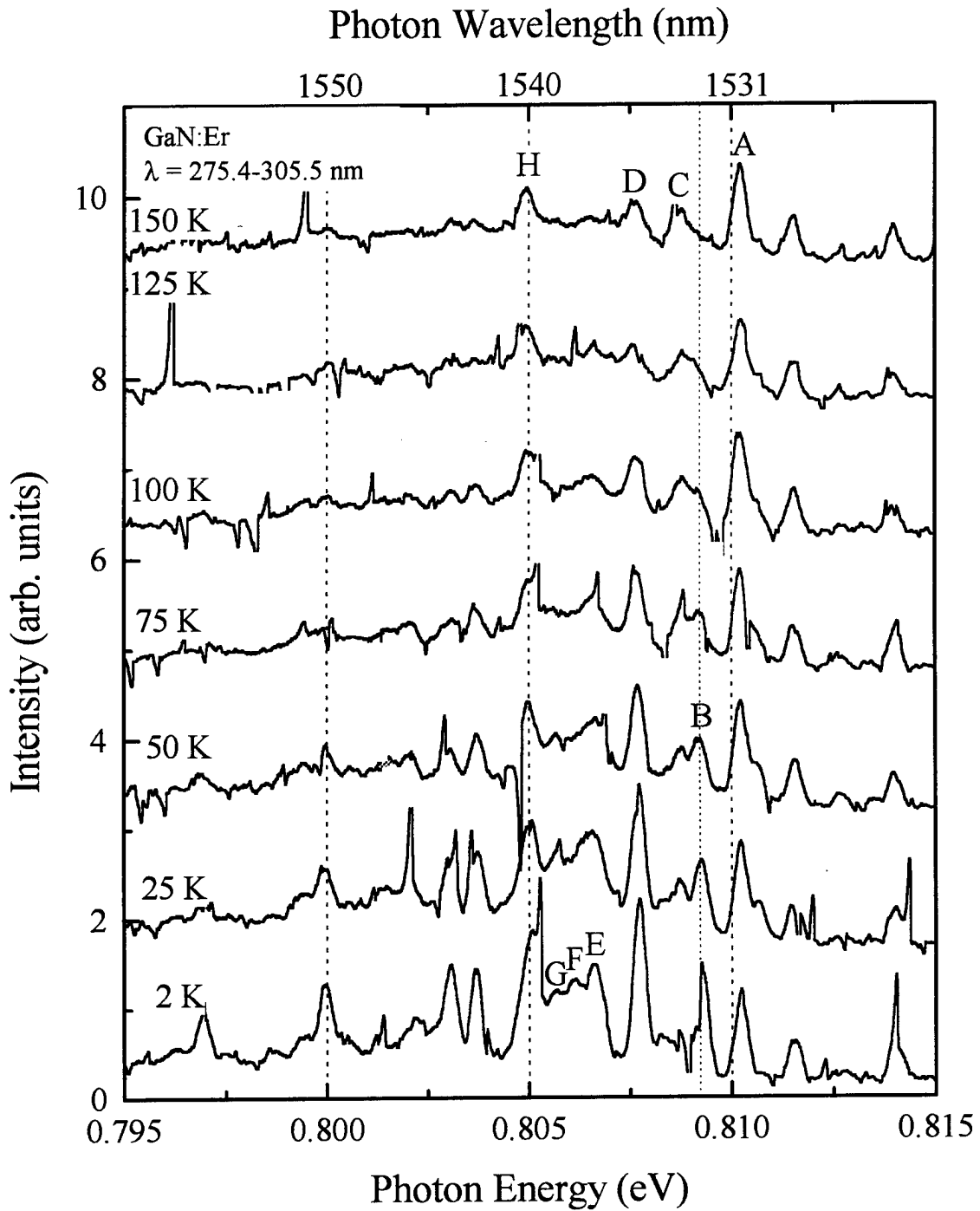


**Figure IV-8.** PL spectra of GaN:Er as a function of sample temperature. Laser excitation wavelength,  $\lambda$ , is 275.4-305.5 nm. Laser power is 400 mW.



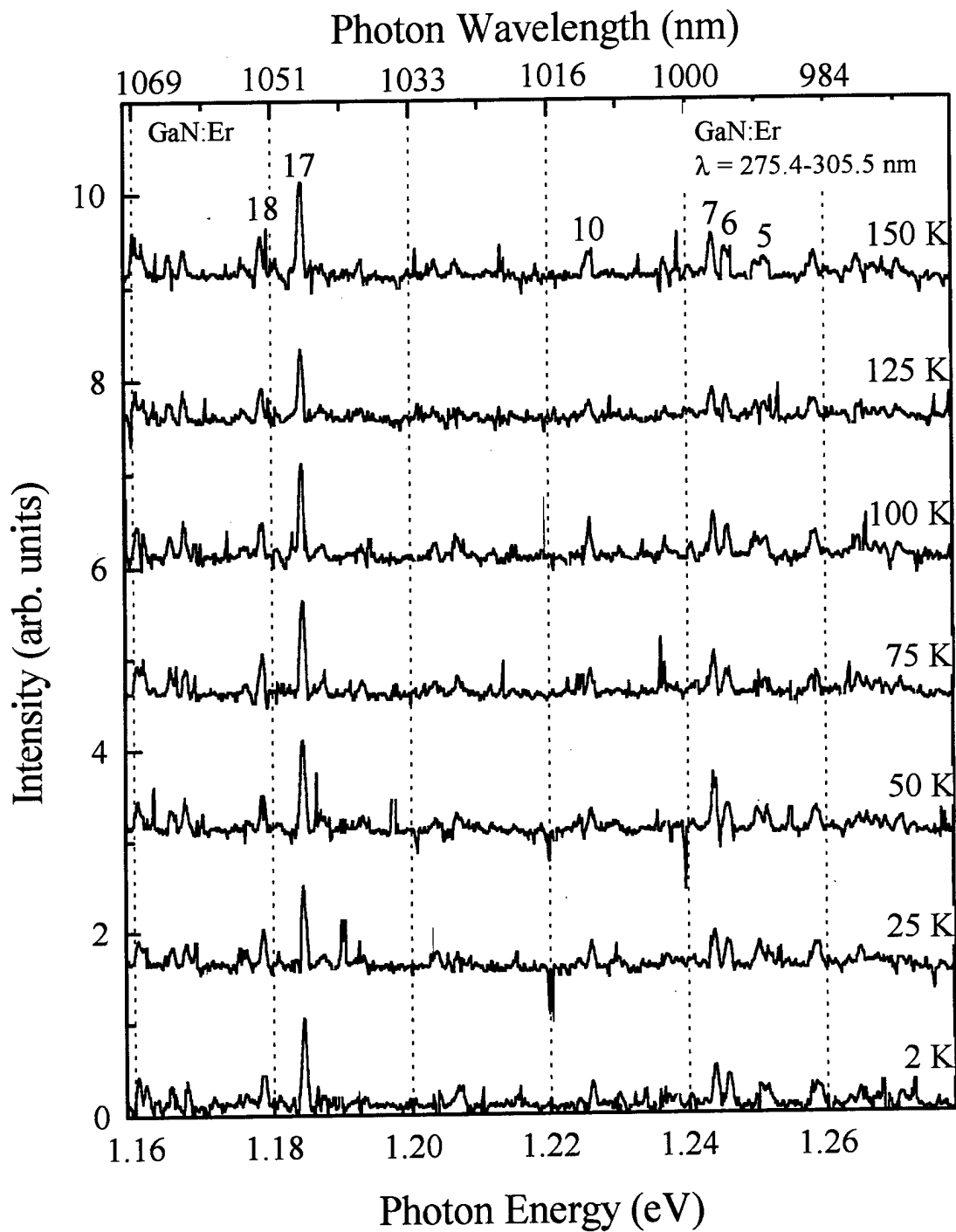


**Figure IV-9.** PL spectra of GaN:Er as a function of sample temperature. Laser excitation wavelength,  $\lambda$ , is 275.4-305.5 nm. Laser power is 400 mW.

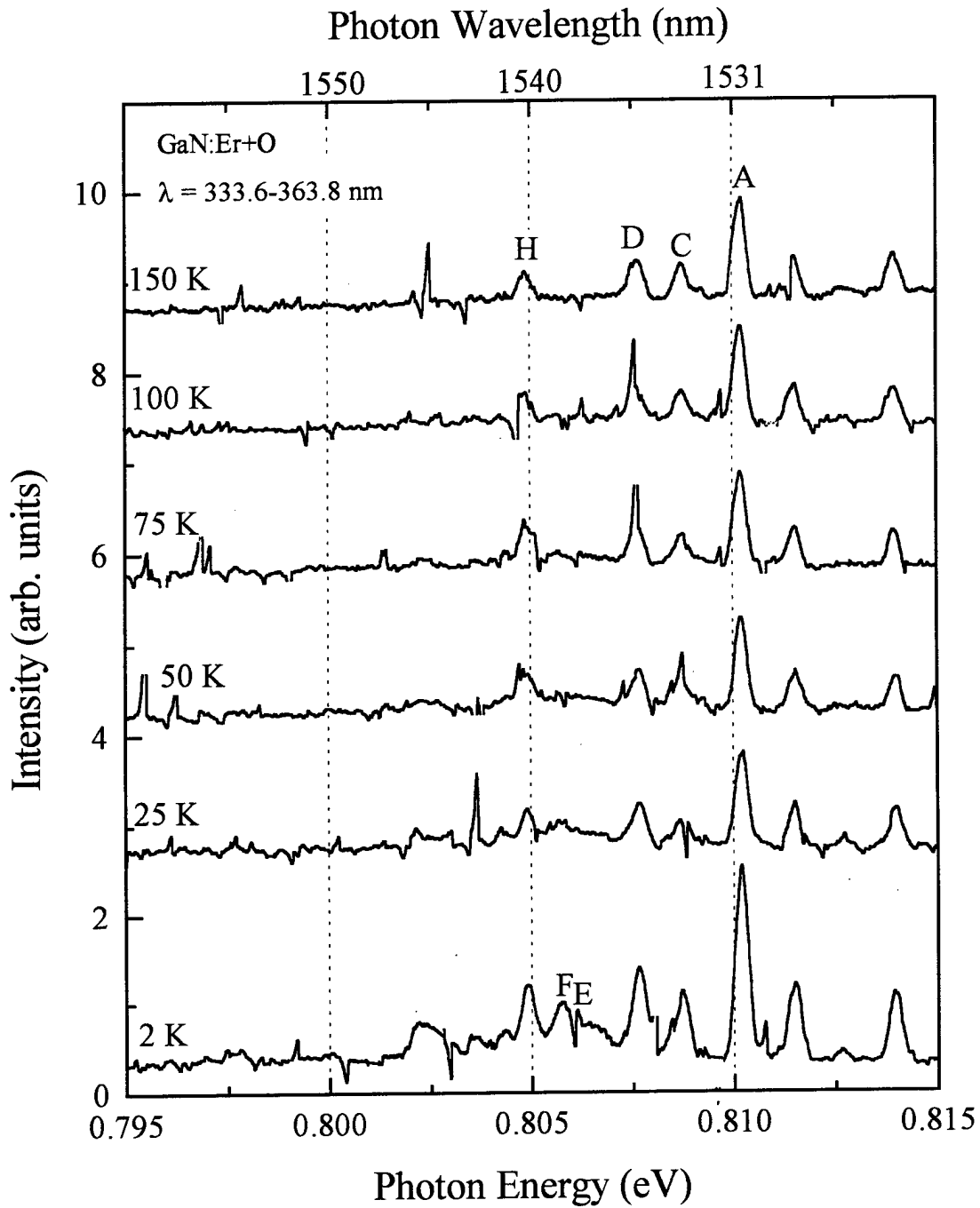


**Figure IV-10.** PL spectra of GaN:Er+O as a function of sample temperature. Laser excitation wavelength,  $\lambda$ , is 333.6-363.8 nm. Laser power is 400 mW.

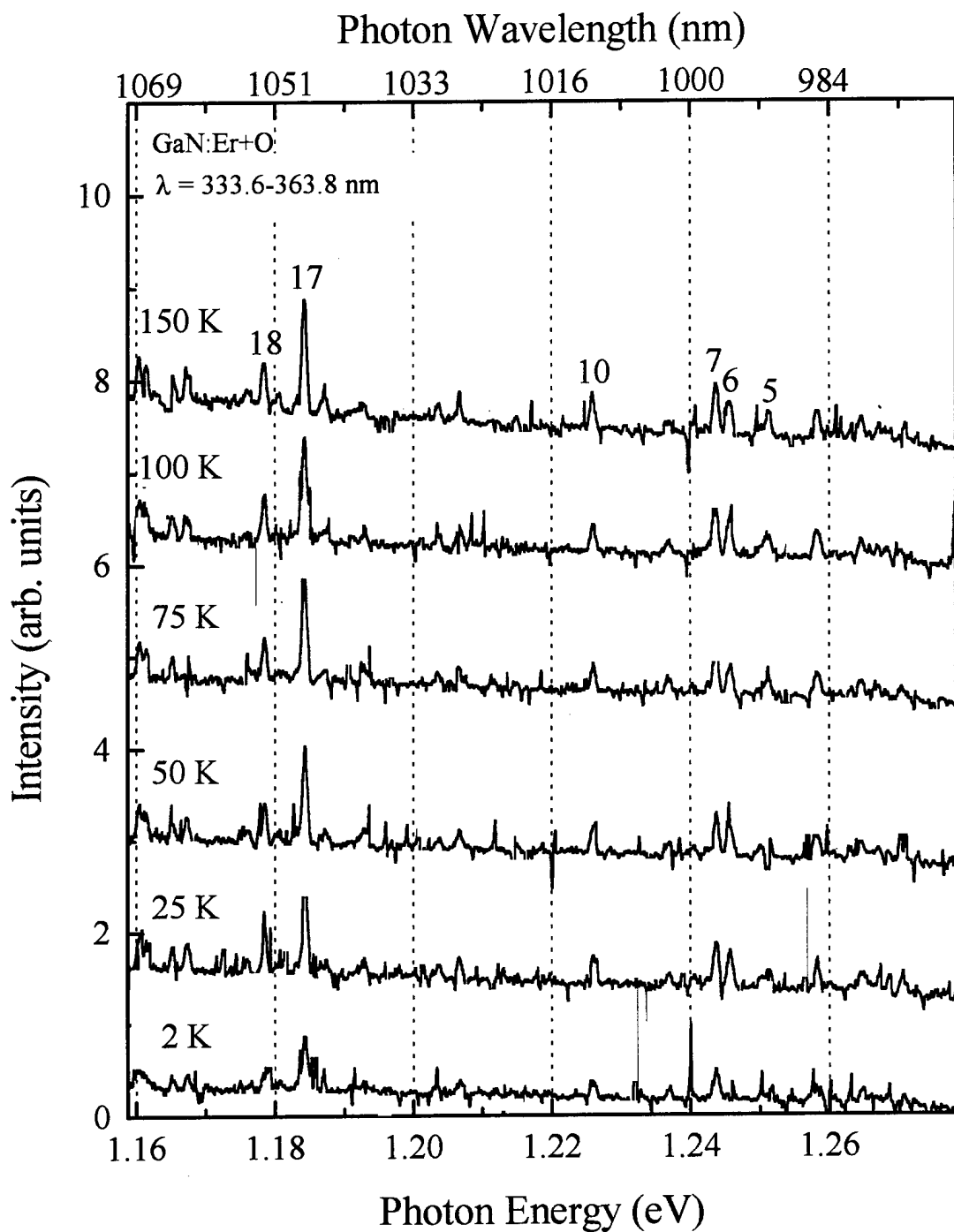


**Figure IV-11.** PL spectra of GaN:Er+O as a function of sample temperature. Laser excitation wavelength,  $\lambda$ , is 333.6-363.8 nm. Laser power is 400 mW

from 2 to 150 K. The emissions around 1.54  $\mu\text{m}$  from sample C decreased by 77% as sample temperature increased to 150 K. On the other hand, the integrated intensity of PL signal around 0.991  $\mu\text{m}$  almost doubled! Once again, the intensity of peaks A, C, D, H, 5-7, 10, 17, and 18 were strong at 150 K.

#### E. Comparison of GaN:Er and GaN:Er+O

This final part compares the PL spectra from GaN:Er to that of GaN:Er+O when the excitation wavelength and sample temperature were varied. Tables IV-4 and IV-5 summarize the integrated intensity emitted from each sample as both the excitation wavelength and sample temperature were varied. Note, the integrated intensity of GaN:Er

**Table IV-4.** Integrated Intensity as a Function of Excitation Wavelength

Sample	Integrated Intensity ( $\text{mm}^2$ ) for Given Excitation Wavelength			
	275.5-305.5 nm	333.6-363.8 nm	488.0 nm	514.5 nm
GaN:Er				
1.54- $\mu\text{m}$ Spectra	971	820	960	984
0.991- $\mu\text{m}$ Spectra	208	189	62	23
GaN:Er+O				
1.54- $\mu\text{m}$ Spectra	552	971	469	340
0.991- $\mu\text{m}$ Spectra	598	628	37	18

was greater when the 275.5-305.5 nm laser line illuminated the sample, but the emissions from sample C were stronger when the 333.5-363.8 nm laser wavelength was used. Oxygen enhanced Er emissions from both the  $^4I_{13/2}$  and  $^4I_{11/2}$  manifolds in GaN when the semiconductor was excited with the 333.6-363.8 nm laser multiline. However, O did not enhance the 1.54- $\mu\text{m}$  transitions when the sample was illuminated with the 275.4-305.5 nm multiline. Furthermore, the integrated intensity of the Er emissions around 1.54  $\mu\text{m}$  from sample B when excited at its optimum excitation wavelength was the same as the integrated intensity induced from sample C at its optimum wavelength, but more photons

were emitted from sample C in the 0.991- $\mu\text{m}$  spectrum than were emitted from sample B at their respective optimum excitation wavelengths.

**Table IV-5. Integrated Intensity as a Function of Sample Temperature**

Sample	Integrated Intensity ( $\text{mm}^2$ ) for Given Sample Temperature		
	2 K	75 K	150 K
GaN:Er			
1.54- $\mu\text{m}$ Spectra	721	579	445
0.991- $\mu\text{m}$ Spectra	180	146	139
GaN:Er+O			
1.54- $\mu\text{m}$ Spectra	572	283	130
0.991- $\mu\text{m}$ Spectra	90	122	173

When sample temperature increased, the integrated intensity of the transitions around 1.54  $\mu\text{m}$  decreased by 38% in sample B and 77% in sample C while the emissions in the 0.991- $\mu\text{m}$  spectra decreased by 22% from sample B but increased by 200% from sample C. In general, the integrated intensity of the 1.54- $\mu\text{m}$  spectra was stronger than that of the 0.991- $\mu\text{m}$  spectra in both sets of experiments, even though the latter spectra included a larger range of wavelengths.

According to Silkowski, peak locations of spectra from GaN:Er and GaN:Er+O are very much the same and oxygen enhances the Er peak at 1.54  $\mu\text{m}$ , but not at 0.991  $\mu\text{m}$ . However, when comparing the PL spectra of the two samples at their best excitation wavelength obtained in this research effort, oxygen enhanced the 0.991  $\mu\text{m}$  peak, but not the 1.54  $\mu\text{m}$  peak. This experiment confirmed Silkowski's claim that peak locations are constant as a function of temperature in GaN:Er and GaN:Er+O, but not about the effects of co-doping on intensity as a function of sample temperature.

In summary, this chapter presents the results of the experiment. First, the transition of an exciton bound to a neutral donor was observed in PL spectra from as-

grown GaN and the transition of an exciton bound to a neutral acceptor may have been revealed. Second, Er peaks were seen at 1.54 and 0.991  $\mu\text{m}$ . Next, PL intensities, but not peak locations, in both doped samples of GaN changed as a function of excitation wavelength. Finally, the PL intensities around 1.54  $\mu\text{m}$  and 0.991  $\mu\text{m}$  persisted in both samples at high temperatures. The next chapter is a more formal conclusion.

## V. Conclusion

This chapter summarizes the results of studying the PL spectra of GaN, GaN implanted with Er, and GaN implanted with Er and O. When GaN was scanned from 350-850 nm, the peak corresponding to the recombination of an exciton bound to a neutral donor was observed at 3.47 eV (357.3 nm) while the energy emitted when an exciton bound to a neutral acceptor recombines may have been 3.457 eV.

Next, the PL spectra from GaN:Er and GaN:Er+O were examined. Erbium electrons made transitions around 1.54 and 0.991  $\mu\text{m}$  in both samples, as in previous work, and the 1.54  $\mu\text{m}$  PL signal remained strong when excited by either above or below bandgap excitation wavelengths. The optimum excitation wavelength was the 275.4-305.5 nm multiline for GaN:Er, but it was the 333.6-363.8 nm multiline for GaN:Er+O. Oxygen enhanced Er emissions from energy states in both the  $^4I_{13/2}$  and  $^4I_{11/2}$  manifolds when the 333.6-363.8 nm laser multiline induced transitions. However, O did not enhance the 1.54- $\mu\text{m}$  transitions when the 275.4-305.5 nm multiline was used.

The final phase measured the PL intensity and peak locations as a function of sample temperature. When sample temperature was increased from 2 to 150 K, the integrated intensity of the transitions around 1.54  $\mu\text{m}$  decreased in both samples; however, the emissions around 0.991  $\mu\text{m}$  from GaN:Er decreased while those from GaN:Er+O doubled. Nevertheless, the PL intensity of the 1.54  $\mu\text{m}$  remained strong at high temperatures. Peak locations shifted no more than 1.239 meV (0.1 nm) as a function of temperature.

This work could not determine whether the PL emissions from either of the doped samples is strong enough to be used in optoelectronic devices because the temperature could not be raised to 300 K, but it did contribute to the knowledge of optical properties of GaN, GaN:Er, and GaN:Er+O. Namely, this work reports the PL spectra from GaN that was excited by above-bandgap energies at 275-4-305.5 nm and scanned near the bandedge (1.46-3.54 eV or 350-850 nm). Moreover, this work studied the PL intensity using two UV lines to excite GaN doped with Er alone and Er and O. Additionally, the effects of changing the sample temperature on PL intensity from GaN:Er and GaN:Er+O were measured while exciting the samples at their respective optimum excitation wavelengths.



### Appendix A: Comparison of Peak Values

This appendix compares Everitt's experimental values of the peaks in the 1515-1575 nm spectral range to published values (Silkowski, 1996:5-141). The UV column is an average of each UV laser line and the visible column is an average of each visible line. Silkowski uses the 514.5 nm line.

Peak	Silkowski (eV)	Silkowski (nm)	Everitt—UV (nm)	Delta (nm)	Everitt—visible (nm)	Delta (nm)
A	0.81017	1530.4	1530.5	-0.1	1530.5	-0.1
B	0.80876	1533.1	1532.2	0.9	1532.2	0.9
C	0.80803	1534.5	1533.3	1.2	1533.6	0.9
D	0.80718	1536.1	1535.1	1.0	1535.1	1.0
E	0.80611	1538.1	1537.2	0.9	1537.2	0.9
F	0.80568	1538.9	1538.3	0.6	1538.1	0.8
G	0.80494	1540.4	1539.1	1.3	1539.3	1.1
H	0.80321	1543.7	1542.8	0.9	1542.8	0.9
I	0.80217	1545.7	1544	1.7	1544.7	1.0
J	0.80151	1546.9	1545.7	1.2	1545.7	1.2
K	0.80103	1547.9	1547.5	0.4	1547.4	0.5
L	0.79957	1550.7	1550	0.7	1549.8	0.9
M	0.79881	1552.2	1551.1	1.1	1551.4	0.8
N	0.79703	1555.6	1554.9	0.7	1554.7	0.9
O	0.7965	1556.7	1555.9	0.8	1555.8	0.9
P	0.79584	1558.0	1557.2	0.8	1557.3	0.7
Q	0.79487	1559.9	1559	0.9	1558.8	1.1
R	0.79425	1561.1	1560	1.1	1560.4	0.7
S	0.79304	1563.5	1562.8	0.7	1562.8	0.7
T	--	--	--	--	--	--
U	0.7917	1566.1	1565.1	1.0	1565.3	0.8
V	0.79088	1567.7	1566.8	0.9	1567.3	0.4
W	--	--	--	--	--	--
X	--	--	--	--	--	--
Y	0.78929	1570.9	1569.8	1.1	1570.6	0.3
Z	0.78801	1573.4	1572.5	0.9	1572.6	0.8

## Appendix B: Peak Locations

The peak locations of transitions between both the  ${}^4I_{13/2} \rightarrow {}^4I_{15/2}$  and  ${}^4I_{11/2} \rightarrow {}^4I_{15/2}$  energy states of Er are listed in this appendix. The  ${}^4I_{13/2} \rightarrow {}^4I_{15/2}$  peaks are listed in part A and the  ${}^4I_{11/2} \rightarrow {}^4I_{15/2}$  peaks are listed in part B. Values are reported to the nearest 1 nm.

### A. Transitions Between ${}^4I_{13/2}$ and ${}^4I_{15/2}$

Peak Location (eV)	Peak Location (nm)
0.8173	1517
0.8157	1520
0.8146	1522
0.8141	1523
0.8130	1525
0.8120	1527
0.8114	1528
0.8104	1530
0.8199	1531
0.8093	1532
0.8083	1534
0.8077	1535
0.8067	1537
0.8062	1538
0.8056	1539
0.8036	1543
0.8025	1545
0.8020	1546
0.8015	1547
0.7999	1550
0.7994	1551
0.7974	1555
0.7968	1556
0.7958	1558
0.7953	1559
0.7948	1560
0.7933	1563
0.7923	1565
0.7913	1567
0.7897	1570
0.7882	1573

**B. Transitions Between  ${}^4I_{11/2}$  and  ${}^4I_{15/2}$** 

Peak Location (eV)	Peak Location (nm)
1.276	972
1.270	976
1.269	977
1.268	978
1.264	981
1.260	984
1.259	985
1.255	988
1.251	991
1.250	992
1.249	993
1.246	995
1.244	997
1.241	999
1.239	1001
1.230	1008
1.228	1010
1.226	1011
1.219	1017
1.214	1021
1.211	1024
1.210	1025
1.208	1026
1.206	1028
1.204	1030
1.200	1033
1.198	1035
1.196	1037
1.192	1040
1.186	1045
1.184	1047
1.181	1050
1.179	1052
1.176	1054
1.169	1061
1.168	1062
1.165	1064
1.162	1068
1.160	1069

## References

- Carrano, J.C. "Very Low Dark Current Metal-Semiconductor-Metal Ultraviolet Photodetectors Fabricated on Single-Crystal GaN Epitaxial Layers," Applied Physics Letters, 70 (15): 1992-1994 (14 April 1997).
- Colon, J.E. "Enhancement of the Er<sup>3+</sup> Emissions from AlGaAs: Er Codoped with Oxygen," Applied Physics Letters, 63 (2): 2277-2279 (12 July 1993).
- Colon, Jose E. Low Temperature Photoluminescence Study of Ytterbium Implanted Into III-V Semiconductors and AlGaAs. MS thesis, AFIT/GEP/ENP/88D. School of Engineering, Air Force Institute of Technology (AU), Wright-Patterson AFB OH, December 1988.
- Ishikawa, Hidenori. "Effects of Surface Treatments and Metal Work Functions on Electrical Properties at p-GaN/Metal Interfaces," Applied Physics Letters, 81 (3): 1315-1321 (1 February 1997).
- Kim, S. "Observation of Multiple Er<sup>3+</sup> Sites in Er-Implanted GaN by Site-Selective Photoluminescence Excitation Spectroscopy." Applied Physics Letters, 71 (2): 231-233 (14 July 1997).
- Nakashima, Kenshiro. "Er-Doping in Silicon By Pulsed Laser Irradiation," Materials Research Society Symposium Proceedings: Rare Earth Doped Semiconductors, 301: 61-65 (1993).
- Pankove, Jacques I. Optical Processes in Semiconductors. New York: Dover Publications, Inc. 1975.
- Silkowski, Eric. Luminescence Study of Ion-Implanted Gallium Nitride. Air Force Institute of Technology (AU), Wright-Patterson AFB OH, November 1996.

## Vita

Captain Lori Everitt was born on [REDACTED]. She graduated with Honors from Shawnee Mission South High School in Overland Park, KS in 1989 and then earned a Bachelor of Science degree in Space Physics at the US Air Force Academy. Upon graduation, she was commissioned as a Second Lieutenant in the US Air Force on 2 Jun 1993. Her first assignment was at the National Air Intelligence Center at Wright-Patterson Air Force Base, OH. There, she worked on routing out threats to the US Air Force mobility aircraft and communicating those threats to policy-makers and operators. She was also part of a joint team which developed threat scenarios in support of Air Force and Army project offices. On 8 Jul 1996, Capt Everitt began the AFIT masters program within the Department of Engineering Physics. Her next assignment is to teach physics at the US Air Force Academy.

Permanent Address: [REDACTED]  
[REDACTED]

**REPORT DOCUMENTATION PAGE**

Form Approved  
OMB No. 0704-0188

Public reporting burden for this collection of information is estimated to average 1 hour per response, including the time for reviewing instructions, searching existing data sources, gathering and maintaining the data needed, and completing and reviewing the collection of information. Send comments regarding this burden estimate or any other aspect of this collection of information, including suggestions for reducing this burden, to Washington Headquarters Services, Directorate for Information Operations and Reports, 1215 Jefferson Davis Highway, Suite 1204, Arlington, VA 22202-4302, and to the Office of Management and Budget, Paperwork Reduction Project (0704-0188), Washington, DC 20503.

<b>1. AGENCY USE ONLY (Leave blank)</b>		<b>2. REPORT DATE</b> December 1997	<b>3. REPORT TYPE AND DATES COVERED</b> Masters Thesis	
<b>4. TITLE AND SUBTITLE</b> Photoluminescence Study of GaN Implanted with Erbium and Erbium+Oxygen			<b>5. FUNDING NUMBERS</b>	
<b>6. AUTHOR(S)</b> Lori R. Everitt, Capt, USAF				
<b>7. PERFORMING ORGANIZATION NAME(S) AND ADDRESS(ES)</b> Air Force Institute of Technology 2950 P St., Bldg 640 Wright-Patterson AFB, OH 45433-7765			<b>8. PERFORMING ORGANIZATION REPORT NUMBER</b>  AFIT/EN/ENP/97D-02	
<b>9. SPONSORING/MONITORING AGENCY NAME(S) AND ADDRESS(ES)</b> AFOSR/NE Physics and Electronics Division Air Force Office of Scientific Research Bolling AFB, DC 20332-0001			<b>10. SPONSORING/MONITORING AGENCY REPORT NUMBER</b>	
<b>11. SUPPLEMENTARY NOTES</b>				
<b>12a. DISTRIBUTION AVAILABILITY STATEMENT</b> Approved for public release; distribution unlimited			<b>12b. DISTRIBUTION CODE</b>	
<b>13. ABSTRACT (Maximum 200 words)</b> Erbium emits at 1540 nm, which propagates well through fiber optic cables. This work studies the photoluminescence (PL) from GaN, GaN implanted with Er alone, and GaN implanted with both Er and O as functions of excitation laser energy and sample temperature. When the exciton bound to a neutral donor recombined, a photon was emitted at 3.47 eV. A photon emitted at 3.457 eV may have been evidence of the recombination of an exciton bound to a neutral acceptor. Second, the Er-ion transitions were observed in two groups around 0.805 and 1.25 eV. The PL intensity was measured at four laser excitation wavelengths of 275.4-305.5, 333.6-363.8, 488.0, and 514.5 nm from an Ar-ion laser. Although the PL intensities from GaN:Er were strongest when the sample was excited by the 275.4-305.5 nm multiline, the PL emissions from GaN:Er+O were strongest when excited with the 333.6-363.8 nm line. Regardless, both above and below bandgap laser lines induced strong PL intensities. Third, PL from the two samples was studied as temperature was increased from 2 to 150 K. In general, the intensities of most peaks decreased as temperature was raised in both samples, but the PL signals persist even at 150 K.				
<b>14. SUBJECT TERMS</b> Gallium Nitride, GaN, Photoluminescence, Wide Bandgap, High Temperature Semiconductors, Rare Earth			<b>15. NUMBER OF PAGES</b> 57	
			<b>16. PRICE CODE</b>	
<b>17. SECURITY CLASSIFICATION OF REPORT</b> Unclassified	<b>18. SECURITY CLASSIFICATION OF THIS PAGE</b> Unclassified	<b>19. SECURITY CLASSIFICATION OF ABSTRACT</b> Unclassified	<b>20. LIMITATION OF ABSTRACT</b> UL	